UNIVERSIDAD
NACIONAL
DE COLOMBIA

Influence of microplastics in the community of benthic foraminifera from a historical perspective

Estefany Andrea Mora Galindo

Universidad Nacional de Colombia
Instituto de Estudios en Ciencias del Mar - CECIMAR
Convenio Universidad Nacional de Colombia - INVEMAR
Santa Marta, D.T.C.H., Colombia
2024

Influence of microplastics in the community of benthic foraminifera from a historical perspective

Estefany Andrea Mora Galindo

Tesis presentada(o) como requisito parcial para optar al título de:
Magister en Ciencias – Biología

Director:

Ph. D. Luisa Fernanda Espinosa Díaz

Co-director:

Dr. rer. nat. Néstor Hernando Campos Campos

Línea de Investigación:

Biología Marina

Universidad Nacional de Colombia

Instituto de Estudios en Ciencias del Mar - CECIMAR

Convenio Universidad Nacional de Colombia - INVEMAR

Santa Marta, D.T.C.H., Colombia

2024

To those who held tight my soul during this adventure.

Acknowledgments

The present research began with a curious interest in marine pollution. Initially, the work of Sara Samaniego inspired me to dive into the issue of plastic pollution. Thanks to her pedagogic project, I became a more conscientious plastic consumer, striving to reduce my usage and ensure recycling. I aspire that every reader of this work continues their efforts to use this versatile material responsibly.

I am grateful to Professor Carlos Alberto Sanchez who encouraged me to tackle this challenge using foraminifera as a tool to explore our environmental history. For some years now, he has guided me in the interesting field of sediment analysis and the study of these remarkable microorganisms. I extend my gratitude to Professor Gladys Rocío Bernal, as well as to Camila Barragan Jacksson, and Lizeth Puerres Torres, for introducing and guiding me in foraminifera picking, differentiation, and patiently addressing my numerous questions. I also wish to express my sincere gratefulness to Sofía Barragán Montilla, a colleague who was always there from the distance to inspire and motivate not only me but also many other female investigators, especially those from Latin America.

Great recognition is due to César Augusto Bernal and Karen Ibarra Gutierrez from INVEMAR whose work and expertise were essential at core collection, slicing, and the subsequent geochemical analyses. For their invaluable assistance and support, I thank Paola Sofía Obando Madera, Juan Fernando Saldarriaga Vélez and Laura Paola Fragozo Velasquez from INVEMAR; without them, the separation of microplastics would not have been possible. I extend heartfelt thanks to all members of CECIMAR who felt like family during this journey; learning from such remarkable marine biology contributors and researchers was enriching. Special thanks to Ivan Alfonso Villamil Martínez and his team at Universidad del Magdalena who facilitated the loss-on-ignition analysis in their laboratory. I want to acknowledge the contribution of the students from the Statistics Department at Universidad Nacional de Colombia who provided their consultation on the statistical analyses; their participation was essential to corroborate the conclusions of this investigation.

Special appreciation goes to the guidance of Luisa Fernanda Espinosa Díaz and Professor Néstor Hernando Campos Campos during the entire investigation process. They consistently motivated me to develop my research skills.

My warmest thanks to my family and friends who supported me every step of the way. Thanks to the great women that joined my road during this challenge; I have no words to express how significant your presence has been in my life. My mother deserves special thanks for planting the seed of curiosity in me from an early age and for playing a key role in the success of the field campaigns. To my father and sister, who stood by my side throughout the entire journey and celebrated every little success. For his unwavering support, I am deeply thankful to Juan Pablo Bayona; his insightful questions and ideas were fundamental in this research, and his constant encouragement kept me going.

This work was possible thanks to cooperation agreement No. 015-2021 with INVEMAR in the framework of RLA 7025 project (*Fortalecimiento de las capacidades en los medios marinos y costeros mediante técnicas nucleares e isotópicas*) financed by the International Atomic Energy Agency (IAEA) and INVEMAR, the resources provided by CECIMAR, and the sponsorship of CEMarin (Call No. 21 of 2020 "*Apoyo financiero a los proyectos de tesis de posgrado en ciencias marinas y afines*").

Abstract

The marine basins have received crescent amounts of plastic since the middle of the last century. Particles smaller than 5 mm are designated microplastics (MPs), and recent studies have revealed that their presence has transformed both the physiochemistry and biology of marine bottoms. To evaluate historical changes in benthic foraminifera and their relationship with the presence of MPs, the composition of the community and the concentration of MPs was evaluated using sediment cores from Ciénaga de los Vásquez, Cartagena, an open marine lagoon. Moreover, core dating analysis was made using ^{210}Pb, which allowed establishing a temporal framework for this study, from 2021±0.31 back to 1961±20.82. The concentrations of MPs reached up to 5358 items/kg in the year 2021±0.31, and a general increase toward the most recent sediments was determined, which reflected global pollution patterns for this material. Although no significant relationship was found between MPs and total carbon and nitrogen, some detailed analyses are suggested to elucidate the historical influence of this pollutant in the sediment chemistry. In addition, variations found in the community of benthic foraminifera (e.g., total abundance, *Ammonia-Elphidium* index, and test morphology) were mostly determined by an increase in organic matter content and a decrease in water energy. Only triserial morphology was explained by the presence of MPs in the sediment. However, both the identification to species level and that of deformed tests are advised since the influence of microplastics might become evident at these finer levels.

Keywords: Microplastic, benthic foraminifera, sediment pollution, historical analysis.

Resumen

Influencia de los microplásticos en la comunidad de foraminíferos bentónicos desde una perspectiva histórica

Las cuencas marinas han recibido cantidades crecientes de plástico desde mediados del siglo pasado. Las partículas menores a 5 mm se denominan microplásticos (MPs), y estudios recientes han revelado que su presencia ha transformado la biogeoquímica y la estructura biológica de los fondos marinos. Para evaluar los cambios en el tiempo de los foraminíferos bentónicos y su relación con la presencia de MPs, se evaluó la composición de la comunidad y la concentración de MPs usando núcleos de sedimento de la Ciénaga de los Vásquez, Cartagena, una laguna marina abierta. Adicionalmente, se realizó datación con ^{210}Pb con el fin de establecer un marco temporal para este estudio, desde el 2021±0.31 hasta 1961±20.82. Las concentraciones MPs alcanzaron valores de hasta 5358 ítems/kg en el año 2021±0.31, y se determinó un aumento general hacia los sedimentos más recientes, lo que reflejó patrones globales de contaminación para este material. A pesar de no hallar una relación significativa entre los MPs y el carbono y nitrógeno total, algunos análisis fueron sugeridos para dilucidar la influencia histórica de este contaminante en la química del sedimento. Además, las variaciones encontradas en la comunidad de foraminíferos bentónicos (e.g., abundancia total, índice *Ammonia-Elphidium*, y morfología de conchilla) estuvieron determinadas principalmente por el aumento del contenido de materia orgánica y la disminución de la energía del medio. Únicamente la morfología triserial fue explicada por la presencia de MPs en el sedimento. Sin embargo, se recomienda la identificación a nivel de especie y de conchillas deformadas ya que la influencia de los MPs podría hacerse evidente en estos niveles más detallados.

Palabras clave: Microplásticos, foraminíferos bentónicos, contaminación sedimento, análisis histórico.

Table of contents

Introduction

For millions of years, marine basins have received sediments from the continents; they have created an environment where numerous species interact and where several biological communities have developed. Among them, benthic foraminifera have registered the environmental characteristics of their surroundings since the Cambrian period and continue to be of great use when studying marine environmental conditions (Jones, 2014).

However, a new material has entered the sedimentary environment in modern times. Since the decade of 1950, the massive production of plastic began, and its durability, versatility, and high resistance made it a popular material (Martin et al., 2020). Unfortunately, insufficient disposal strategies have led to the incursion of this material into the ocean in great abundance and speed; approximately 5-8 million tons of plastic enter the ocean every year (Birarda et al., 2021). Notably, several researchers report novel rock types such as plastiglomerates and quartz plastisandstones (Galloway et al., 2017; Martin et al., 2022; Rangel-Buitrago et al., 2023; Rangel-Buitrago & Neal, 2023).

Among the variety of plastic particles that enter the sediment, those smaller than 5 mm are regarded as microplastics (MPs) (Frias & Nash, 2019). After falling to the seabed, they affect both the normal composition and configuration of the sediment and the species that inhabit it (Birarda et al., 2021; Carson et al., 2011; Hope et al., 2020; Ladewig et al., 2021; Moore, 2008; Nelms et al., 2016; Seeley et al., 2020; Wang et al., 2022; Yao et al., 2019).

Particularly, Bouchet et al. (2023) indicate that the effect of MPs in foraminifera can be assessed from three different approaches: cellular (comprising cellular alterations and physiological changes), individual (including motion and behavior), and community levels (focusing on the composition of foraminiferal communities). For instance, Birarda et al., (2021) found clear evidence of oxidative stress and metabolic depression of some foraminifera species when exposed to a plastic derived compound and associated to living attached to plastic surfaces. They found a high propensity to accumulate synthetic molecules in the cytoplasm and test of the calcareous foraminifera, and they found evidence of MP incorporation in agglutinated tests. Moreover, Grefstad (2019) found that foraminifera can

ingest and accumulate MPs of diverse sizes leading to their transfer to the food web. Recently, Plafcan et al. (2024) found increasing inclusion of MPs in agglutinated foraminifera associated with their increase in the sedimentary record.

The current work evaluated the influence of this pollutant on both the sediment and belongs to the first steps in evaluating its effect on the benthic foraminifera at the community level from a historical perspective. For this aim, the analyses were made on sediment cores from Ciénaga de los Vásquez, an open marine lagoon in Cartagena, Colombia. Accordingly, Chapter 1 deals with the concentration of MPs over time and in relation to carbon and nitrogen contents in the sediment. Chapter 2 presents the changes in the benthic foraminifera community over time. Lastly, Sections 3 and 4 present the final discussion, conclusions, and recommendations, where the influence of MPs on the benthic foraminifera is evaluated.

Study area

The coastal lagoon Ciénaga de los Vásquez, Cartagena, Colombia is one of six lagoons in Barú, and it is the closest to the Cartagena Bay. It has a wide entrance of about 460 m with no barrier islands, presents a central narrowing of about 60 m, and the total length from the entrance to the innermost margin is about 1350 m. The total area is 310,254.7 m^2. This lagoon was selected because despite its proximity to the Dique channel, an artificial arm of the Magdalena River (see sediment discharge north and south of the lagoon in Figure 1), no freshwater flows into the lagoon (Parada Ruffinatti et al., 1996), which presumably makes it a great scenario to evaluate MPs in the sea.

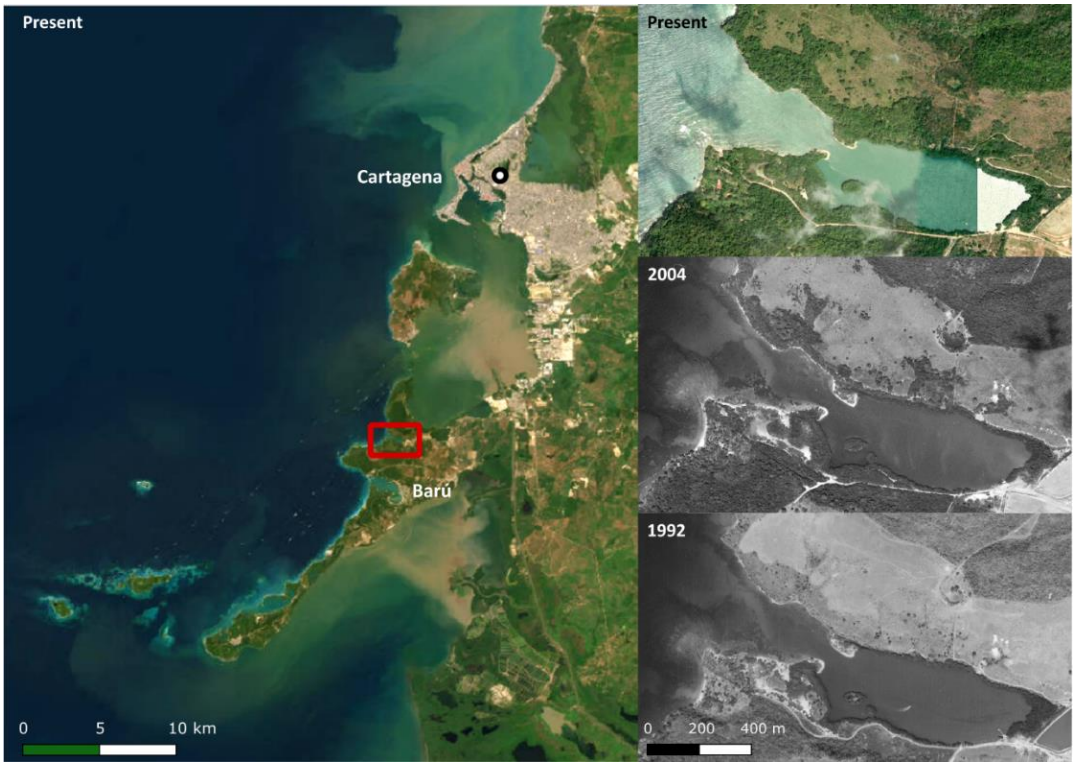

Figure 1. Left: Location of Ciénaga de los Vásquez in relation to Barú island and Cartagena (red square). Right: Aerial views of the lagoon from 1992, 2004, and present (2021). Satellite images from Esri (https://www.arcgis.com/home/item.html?id=10df2279f9684e4a9f6a7f08febac2a9); aerial photographs (black and white) taken from IGAC (Photo C-2469-0215 for 1992, and C-2712-0082 for 2004; from https://www.colombiaenmapas.gov.co/).

Parada Ruffinatti et al. (1996) indicated that Ciénaga de los Vásquez has little to no influence of the Magdalena River due to the following findings:

1. The physicochemical properties of the water remained relatively constant among their multi-seasonal measurements, which was associated with its direct and broad communication to the sea.
2. Quartz grains in the sediment were angulous and lustrous, which indicates a neighboring source area, probably a deposit of siliceous gravel close to Cartagena, according to these authors. Conversely, sediments sourced from the Magdalena River present round shapes and dull surface due to the long transport.
3. The lagoon's water temperature in the west side of Barú was in average 29.7 °C. That of those on the east side of Barú was 31.3 °C; such higher temperatures were associated to the warm water supply of the river.
4. The organic matter (OM) content was the highest in the lagoons in the east of Barú and progressively decreased clockwise toward Ciénaga de los Vásquez; the Magdalena River

was identified as the source of OM indicating that those lagoons in the west side receive negligible influence of the river. In contrast, calcium carbonate was the highest in Ciénaga de los Vásquez and decreased anticlockwise to the eastern lagoons; local erosion of neighboring reefs and the Pleistocene-Pliocene Fm. La Popa Superior (fossil reefs) was attributed to this finding.

Barú undergoes rainy and dry seasons from August to November and from December to April, respectively; the movement of the Intertropical Convergence Zone in the Colombian Caribbean causes this climatic pattern. According to Parada Ruffinatti et al. (1996), during the dry season, the Trade Winds and waves strongly impact the northern entrance of Ciénaga de los Vásquez, eroding it in a NNE direction. During the rainy season, the wave direction changes, distributing coarse sediments along the southern part of the lagoon (Miranda & Parada Ruffinatti, 1987). The rocky coastline in the northern entrance of the lagoon and the sandy coastline in the south, confirm this pattern.

In the innermost area of the lagoon, fine clayey sediments prevail, indicating low energy and *in situ* sedimentation (Miranda & Parada Ruffinatti, 1987) with a rate of 1 cm every 1.5 years based on living foraminifera, total assemblage, and their reproduction rate (Parada Ruffinatti et al., 1996). In addition, as shown in Figure 1, there have been no significant changes in the geomorphology of the lagoon since 1992, and according to Parada Ruffinatti et al. (1996), there had been no significant changes since 1983. However, some increase in the surrounding vegetation density, which consists of mangroves, is apparent. No reports of dredging activity, trawling fishing, anchorage or transit of vessels propelled with poles on the seabed have been found. Moreover, the lagoon is not known as a touristic attraction.

Given the absence of studies conducted in this lagoon since the previous century, the potential impact of escalating plastic pollution on it has prompted the need for this research. The abundance of foraminifera and the earlier investigations offer a valuable foundation for this assessment.

1. Temporal variations of microplastic concentration in Ciénaga de los Vásquez

1.1 Abstract

Microplastics (MPs) were extracted from a sediment core from an open marine lagoon in a Colombian coastal lagoon, Ciénaga de los Vásquez, Cartagena, to analyze changes in concentration over time and evaluate their influence in sediment chemistry. A historical framework was achieved through ^{210}Pb core dating analysis. Nile Red-induced fluorescence of MPs under 365 nm light and automatic counting with ImageJ allowed for a cheap and time-effective assessment of MP concentration and detection of particles down to 44.27 μm. The concentration of MPs reached up to 5358 items/kg d.w. in the year 2021±0.31 and has increased over time reflecting global pollution patterns for this material. Most MPs along the core were small (95% < 299 μm), representing a commonly overlooked size range by conventional methodologies. Moreover, no significant correlation was found between MP concentration and total carbon and nitrogen; however, more specific analyses such as organic and inorganic carbon and inorganic and organic nitrogen species are recommended to gain comprehensive understanding on the historical influence of this pollutant on sediment characteristics. These results constitute the first report along Colombian coasts of MP concentrations over time using a sediment core.

1.2 Introduction

Microplastics (MPs) are plastic particles smaller than 5 mm (Frias & Nash, 2019), and the concern about them as a pollutant has raised exponentially since the 1970s on their first report in plankton net samples (Colton Jr et al., 1974). These particles are both manufactured in those sizes for cosmetic, industrial, pharmaceutical applications, among others, known as primary MPs (Galloway et al., 2017); and also generated by the fragmentation of bigger plastic pieces through processes like photodegradation, thermo-oxidative degradation, hydrolysis, and microbial attack, known as secondary MPs (Rogers et al., 2020).

The distribution of MPs in the ocean is determined by natural factors such as marine and wind currents, as well as anthropogenic drivers including the location of industrial and urban centers that discharge these particles in coastal settings (Acosta-Coley et al., 2019; UNEP, 2016; Yao et al., 2019). Their deposition in ocean bottoms is influenced by their size, shape, polymer type, the formation of biofilms, and the ingestion and defecation from organisms (Galloway et al., 2017; Rogers et al., 2020).

MPs are then incorporated into the sedimentary record and persist there for extended periods (Rangel-Buitrago & Neal, 2023); between 70% and 90% of MPs accumulate in the sediments (Uddin et al., 2021). Typically, studies on sediment cores have found the highest concentrations of these particles in the topmost ~15 cm with exponential decrease toward the deeper layers of sediment (Garcés-Ordóñez et al., 2022; Mai et al., 2018; C. Martin et al., 2020; Zheng et al., 2020). Notably, Garcés-Ordóñez et al. (2022) underlined the need to advance in the quantification of smaller MPs (<200 μm), which seem to comprise a significant portion of the plastic pollution in marine environments.

Several authors suggest that the presence of MPs in the sediment affects the normal functioning of the carbon cycle through several processes: its use as a carbon source by certain microorganisms (Ladewig et al., 2021), the disruption of plant and animal activities and their gene abundance and enzyme activity (Wang et al., 2022), the leaching of dissolved organic carbon, and the modification of microbial communities (Rogers et al., 2020), among others. For instance, a study in the East China Sea, concluded that the continuous accumulation of MPs in marine sediments might result in overestimation of organic carbon storage because MPs are carbon dominated anthropogenic materials and may represent a hidden contribution to carbon burial(Lin et al., 2021). Moreover, MPs can also impact the nitrogen cycle by affecting

nitrogen storage, nitrification, and denitrification processes (Hope et al., 2020; Ladewig et al., 2021; Muthu, 2021; Seeley et al., 2020; Wang et al., 2022).

The deficient waste management in Latin America is highly responsible for plastic pollution; only ~4% of the plastic is recycled, and around 71% of all generated MPs are secondary (i.e., derived from poor waste management); particularly, in Colombia only 30.6% of the population has access to municipal waste management services, and separation of plastic waste in the source is inadequate (Kutralam-Muniasamy et al., 2020). . For instance, Rangel-Buitrago et al. (2021b) stated that in 2019 only 17% of the litter generated in Colombia was recycled.

Moreover, the Magdalena River discharges an estimated amount of 16,700 tons of plastic to the sea every year in the Colombian Caribbean (Lebreton et al., 2017). This region exhibits the highest concentrations of MPs in sediments among coastal regions in Colombia, principally in Cartagena and Santa Marta, where up to 2863 items/kg has been reported in coastal sediments (Galindo et al., 2023; Garcés-Ordóñez et al., 2019). Particularly, Cartagena is known as a production center of plastics with several petrochemical facilities, generating large amounts of primary MPs (Acosta-Coley et al., 2019).

This study aims to provide the first report of microplastic concentrations over time for the Colombian Caribbean, in a coastal lagoon, Ciénaga de los Vásquez, Cartagena, and evaluate the relationships between the concentration of this pollutant and carbon and nitrogen contents in the sediment. It is expected that this work encourages future studies in sedimentary records to understand the history of plastic deposition in various coastal settings in Colombia.

1.3 Methods

Two sediment cores were collected in April 2022, in the central part of the lagoon where *in situ* sedimentation takes place (Miranda & Parada Ruffinatti, 1987; Parada Ruffinatti et al., 1996) (Figure 2, Table 1). Each core was manually obtained using a transparent acrylic pipe 8.6 cm inner diameter and 120 cm length. Core A1 was selected for MPs and abiotic measurements (this chapter), whereas core A2 for foraminifera analyses (Chapter 2).

Table 1. Recorded core locations, water depth, and lengths at sampling sites.

Core	Coordinates	Water depth (m)	Core length
A1	10° 15' 44.1'' N 75° 35' 10.4'' W	3.2	94 cm
A2	10° 15' 43.9'' N 75° 35' 10.0'' W	3.2	88 cm

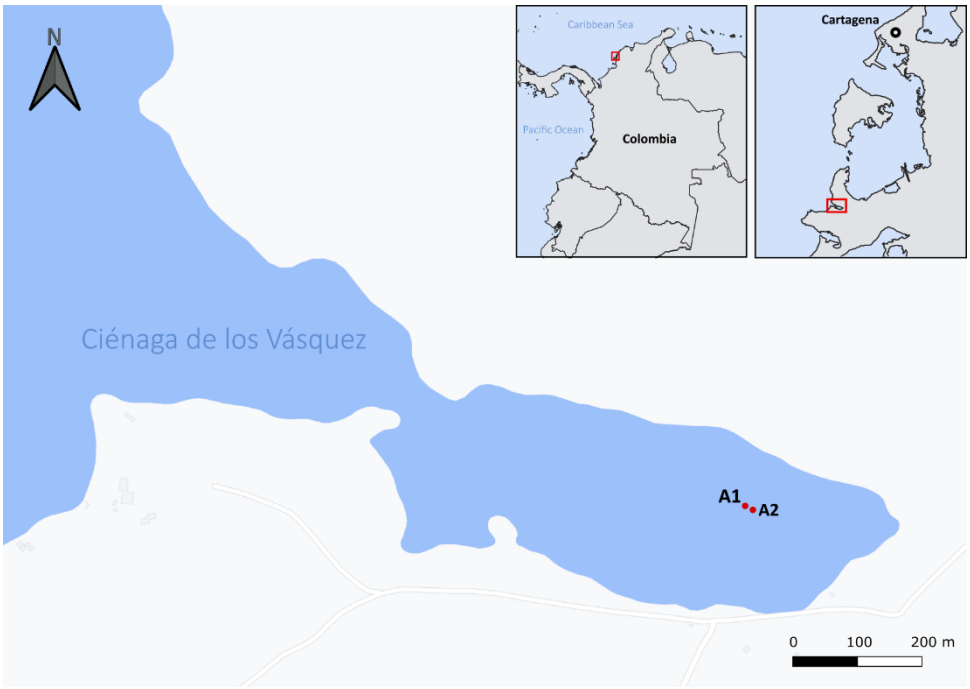

Figure 2. Location of Ciénaga de los Vásquez and sediment core sample locations (A1 and A2). The distance between the cores is 13.5 m.

In situ measurements such as water depth, and the parameters salinity, dissolved oxygen, temperature, and pH, were taken at core A1 location in the surface water, using a digital multiparameter portable meter (WTW™, Multi 3630 IDS) (INVEMAR, 2003). These parameters were measured to further confirm whether marine conditions still prevail in the area as stated by Parada Ruffinatti et al. (1996).

Each core was extruded and sliced into 1-cm intervals according to IAEA (2021), and stored at -20 °C prior to analyses (the sections are hereafter referred to as "samples"). During sampling and core slicing, cotton clothes and lab coats were used to prevent MPs contamination (Prata et al., 2019a). Moreover, all sampling equipment was washed with MilliQ® water prior to sampling.

All core A1 samples were dried at 45 °C; this temperature was used to prevent ^{210}Po volatilization, which occurs at 60 °C, and to prevent organic carbon loss (IAEA, 2021). This procedure took around two weeks; thereafter, weight measurements were taken at 24-hour intervals until the weight variation was less than 5%. The dry weight was recorded at that point (Appendix A, Table A1).

Each sample was macerated in an agata mortar before core dating, and total carbon (TC), and total nitrogen (TN) analyses.

1.3.1 Core dating

The core A1 was dated at the Marine Environmental Quality Laboratory (LABCAM) of INVEMAR using ^{210}Pb method, which is known for its high resolution in dating sediments approximately within a one-hundred-year period (IAEA, 2012). Eighteen samples were analyzed throughout the core (Table 2). The total ^{210}Pb activity was assessed through its daughter product ^{210}Po with an alpha particle spectrometer (ORTEC Alpha Ensemble model, with hyper pure silicon detector) in 0.5 g of dry sediment (dried at 45°C, macerated and sieved through 250 μm) (Sanchez-Cabeza & Ruiz-Fernández, 2012; Toro et al., 2021). All samples were digested with HNO_3, HCl, and HF; thereafter Po was deposited on silver disks in presence of HCl (IAEA, 2012). The reference material for ^{210}Pb was DL1-A (Uranium-Thorium Ore DL1-A, Canada Centre for Mineral and Energy Technology). Supported ^{210}Pb was calculated by averaging total ^{210}Pb at the base of the core where it reached a constant activity, i.e., from the sample 59-60 cm depth to the bottom of the core (Table A2). The excess ^{210}Pb was calculated as the subtract of total and supported ^{210}Pb using the constant flux–constant sedimentation model (CF:CS) (Krishnaswamy et al., 1971). This model implies assuming a constant net rate of supply of unsupported ^{210}Pb from the atmosphere and a constant sedimentation rate.

Table 2. Analysis per sample in core A1. MPs: Microplastics, ^{210}Pb: Core Dating, TC: Total Carbon, TN: Total Nitrogen.

Depth	Drying	MPs	^{210}Pb	TC	TN	Depth	Drying	MPs	^{210}Pb	TC	TN
0-1	X	X		X	X	47-48	X		X		
1-2	X	X	X			48-49	X				
2-3	X	X		X	X	49-50	X				
3-4	X	X		X	X	50-51	X	X	X	X	X
4-5	X	X		X	X	51-52	X				
5-6	X		X			52-53	X				
6-7	X	X		X	X	53-54	X				
7-8	X					54-55	X		X		
8-9	X					55-56	X				
9-10	X	X				56-57	X				
10-11	X					57-58	X				
11-12	X	X		X	X	58-59	X		X		
12-13	X		X			59-60	X		X		
13-14	X	X				60-61	X	X		X	X
14-15	X	X		X	X	61-62	X		X		
15-16	X					62-63	X				
16-17	X	X		X	X	63-64	X				
17-18	X					64-65	X				
18-19	X					65-66	X				
19-20	X	X		X	X	66-67	X				
20-21	X					67-68	X				
21-22	X					68-69	X				
22-23	X					69-70	X				
23-24	X					70-71	X	X	X	X	X
24-25	X	X	X	X	X	71-72	X				
25-26	X					72-73	X				
26-27	X					73-74	X				
27-28	X					74-75	X		X		
28-29	X					75-76	X				
29-30	X	X				76-77	X				
30-31	X					77-78	X		X		
31-32	X		X			78-79	X				
32-33	X					79-80	X				
33-34	X					80-81	X				
34-35	X	X		X	X	81-82	X				
35-36	X					82-83	X				
36-37	X					83-84	X				
37-38	X					84-85	X		X		
38-39	X					85-86	X				
39-40	X	X		X	X	86-87	X				
40-41	X					87-88	X				
41-42	X					88-89	X		X		
42-43	X					89-90	X				
43-44	X					90-91	X				
44-45	X	X	X	X	X	91-92	X				
45-46	X					92-93	X		X		
46-47	X					93-94	X				

1.3.2 Microplastic content

Microplastic separation

Twenty (20) sediment samples from the core were used and separation of MPs was made following the methodology of Research Network of Marine-Coastal Stressors in Latin America and the Caribbean-REMARCO (IAEA, Technical Doc in construction). As shown in Table 2, most analyses were concentrated within the initial 20 cm, covering the first 5 cm completely; several studies have reported the highest concentration of this pollutant in this portion of the sedimentary record (Hidalgo-Ruz et al., 2012; Mai et al., 2018; Prata et al., 2019a; Zheng et al., 2020).

The analysis was made in two badges of 10 samples. The organic matter (OM) removal from sediment was done with hydrogen peroxide (H_2O_2, 30%) and Fenton solution. Density separation was made with saturated sodium chloride solution (NaCl, 1.2 g/ml) (Figure 3). The filtration step was made with 47 mm-diameter 0.7 µm-pore size glass microfiber filters (GF/F No 1825-047, Whatman®), previously combusted at 550 °C. To prevent both false positives in MPs count, and to remove biofilms from the MPs, an extra OM removal step was made in the filters using piranha solution. The solution was left to react for 1 min and then thoroughly rinsed with MilliQ® water (0.22 µm filtered) (Lavoy & Crossman, 2019; Liu et al., 2022; Meyers et al., 2022; Prata et al., 2019b; Yao et al., 2019).

Figure 3. Density separation of MPs using NaCl saturated solution. The sediment can be seen on the bottom of the beakers, while MPs remain on the surface.

To prevent count errors caused by cross-contamination, all work was conducted in clean rooms, with controlled air circulation, closed doors and windows, and limited personal circulation (Rocha-Santos et al., 2022); moreover, one procedural blank and one duplicate were run for each badge (Table A3). Solution preparation and materials pre-wash (principally of glass and metal) were performed using MilliQ® water, and a cotton lab coat was worn during all processing steps (Frias et al., 2018).

Microplastic count

After processing the samples, microplastics were counted to report them in items/kg (d.w.). This was performed with the aid of Nile red (NR) solution, which has gained popularity in recent years since it eases the identification of MPs in environmental samples by making them acquire fluorescence under certain wavelengths (Capolungo et al., 2021; Liu et al., 2022). The advantages of this methodology in combination with computerized image analysis, for counting purposes, have been reported by several authors (Capolungo et al., 2021; Liu et al., 2022; Meyers et al., 2022; Prata et al., 2019b).

NR solution was prepared dissolving 1 mg of NR (technical grade, N3013, Sigma-Aldrich) in 1 ml acetone (99.5 %) and brought to a final volume of 100 ml with ethanol (70%) instead of MilliQ® water (as suggested in the REMARCO's methodology); the concentration was thus 10 µg/ml as recommended by Liu et al. (2022) and Prata et al. (2020a). Ethanol was used because NR is a hydrophobic dye and the partitioning of its molecules to plastics is less effective with water; the fluorescence and thus recovery rate of MPs are dependent on solvent nature (Liu et al., 2022). The use of ethanol has been reported in several studies of MPs analysis (Meyers et al., 2022; Prata et al., 2020b; Prata et al., 2019b). NR was added to each filter (immediately after digestion with piranha solution and rinse with MilliQ® water) and left to react for 5 min (Prata et al., 2020a); then, each filter was thoroughly rinsed with MilliQ® water and vacuum filtered to prevent NR residues and accumulations (Meyers et al., 2022).

Subsequently, the filters were placed in labeled glass petri dishes, covered with aluminum foil and oven-dried at 60 °C. The aluminum foil prevented light and environment MPs from entering the petri dish (Figure 4). The samples were stored in complete darkness conditions before the counting procedure.

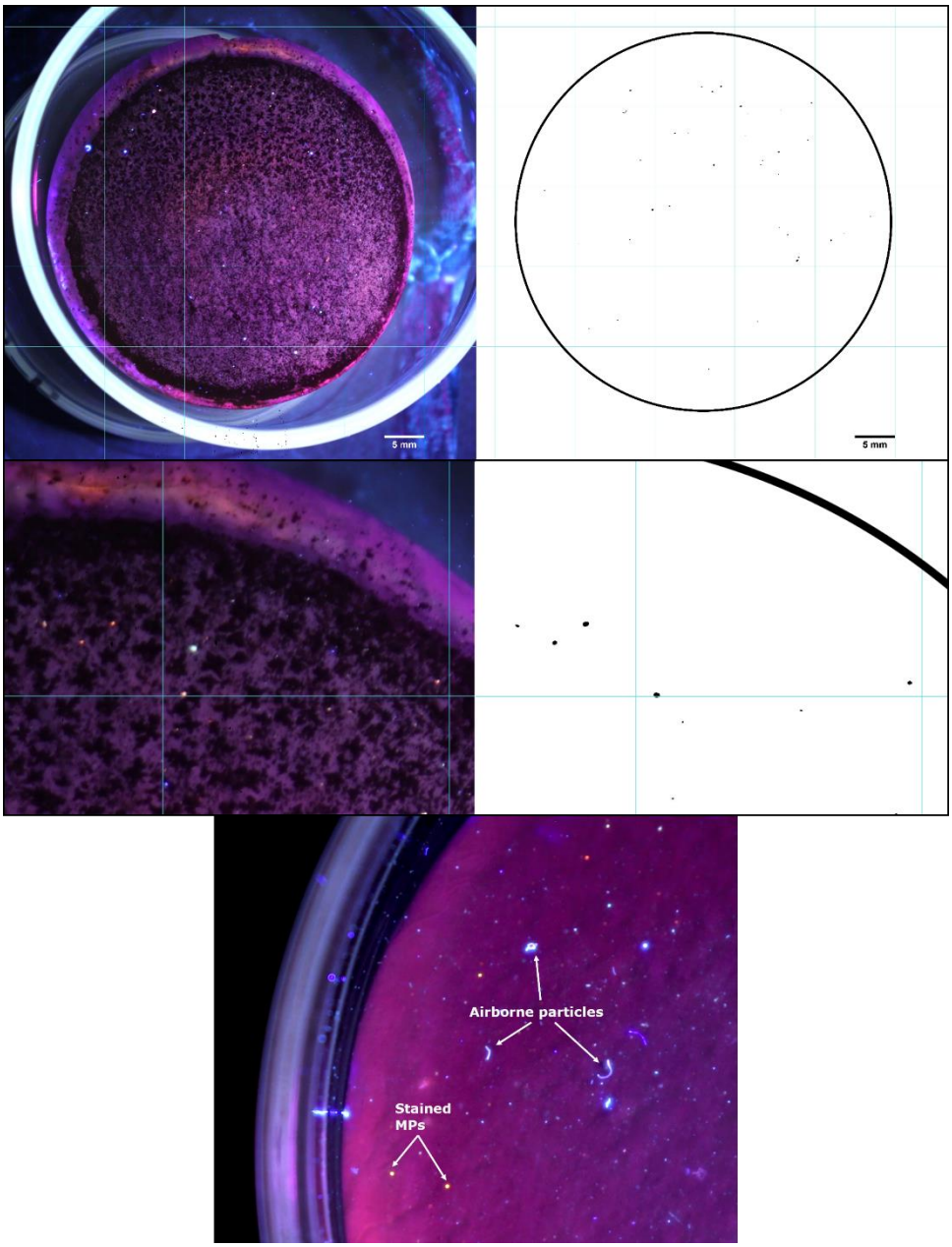

Figure 4. First row: Photography of sample 9-10 cm showing Nile red-stained MPs and the mask image produced by MP-VAT 2.0A that presents the detected and automatically counted particles. Second row: zoom of the first photograph. Third row: sporadic airborne fibers or particles (on test sample) presenting strong blue reflection of the light, which increased in time with the open petri dish.

Thereafter, all filters were photographed with a Canon Rebel T7i under 365 nm light in a dark room under constant room temperature and no air currents. Photograph conditions were set at ISO 100, F5.6, WB in Tungsten mode, and 2s of exposure, keeping focus and stabilization constant (Prata et al., 2020a).

As suggested by Prata et al. (2020a), one darkframe photograph was taken for each sample badge to remove camera noise and defects from sample photographs using the Defect Eraser macro in the ImageJ free software (http://imagej.nih.gov). Following defect removal, MPs counting was performed using a modification of the MP-VAT 2.0 script (macro proposed by those authors) in ImageJ. See Appendix B for the modified script MP-VAT 2.0A.

MP-VAT 2.0 allows the automatic quantification of microplastics with a recovery rate of 95.9%±10.3 for environmental samples (Prata et al., 2020a) and counts red reflections of the image, which correspond to MPs, as shown in Figure 4. The modifications made for this study are presumed to uphold the recovery rate of the original script (See Appendix B). Additional modifications were made to the script to include grid and scale in the mask image easing comparison with the original photo (Figure 4) and to automatically store the mask image in photo file location.

For setting the scale of the photos using filter's diameter, and thus allowing measurement of MPs, prior use of MP-Scale macro (Prata et al., 2019b) was required. A modified version of this script was made (Appendix B), which, in addition, stores a copy of the original photograph with grid and scale to ease comparison with the mask image generated from MP-VAT 2.0A.

All photography sessions took place in the same week of the staining process because physical samples tend to loose particles after the separation, and fluorescence is prone to get lost after a couple of months (Prata et al., 2020a).

1.3.3 Geochemical analyses (TC, TN)

TC and TN analyses were made to gain insights on MP influence on sediment chemistry. These were performed by LABCAM on 20 samples (Table 2) using dry oxidation and quantification by elemental analysis (Thermo Scientific, Flash smart- CHNS/O analyzer). For TC analysis, the methods ISO 11464 (2006) and modified ISO 10694 (1995) were used; for TN, ISO 11464 (2006) and modified ISO 13878 (1998) were used. The samples were chosen to match those of MPs analysis.

1.4 Results

At core A1 location (Table 1) the water salinity was 34.5, dissolved O_2 concentration was 7.63 mg/L, temperature was 29.5 °C, and pH was 8.13. *In situ* measurements were not taken at core

A2 location due to the proximity to core A1. The results of core dating and MPs are presented in the following subsections.

1.4.1 Age model (Chronology of the sediment core)

The total activity of ^{210}Pb showed an exponential decay with mass depth throughout core A1 as shown in Figure 5. Supported ^{210}Pb activity was 11.5 Bq kg^{-1}, and was estimated by averaging $^{210}Pb_{tot}$ activities at the base of the core where it reached constant behavior (from the sample 59-60 down to the bottom of the core) (Zaborska et al., 2007). Consequently, a reliable sediment chronology of around 60 years was achieved for the top 59 cm of the sediment core, (Figure 5). The sediment chronology was calculated from the constant flux-constant sedimentation model (CF:CS) (Krishnaswamy et al., 1971), where the corresponding mass accumulation rate was 0.597 g cm^{-2} yr^{-1}, and the sediment accumulation rate was 0.967 cm yr^{-1}. Therefore, temporal estimation was possible from 2021±0.31 back to 1961±20.82. For detailed results, refer to Table A2.

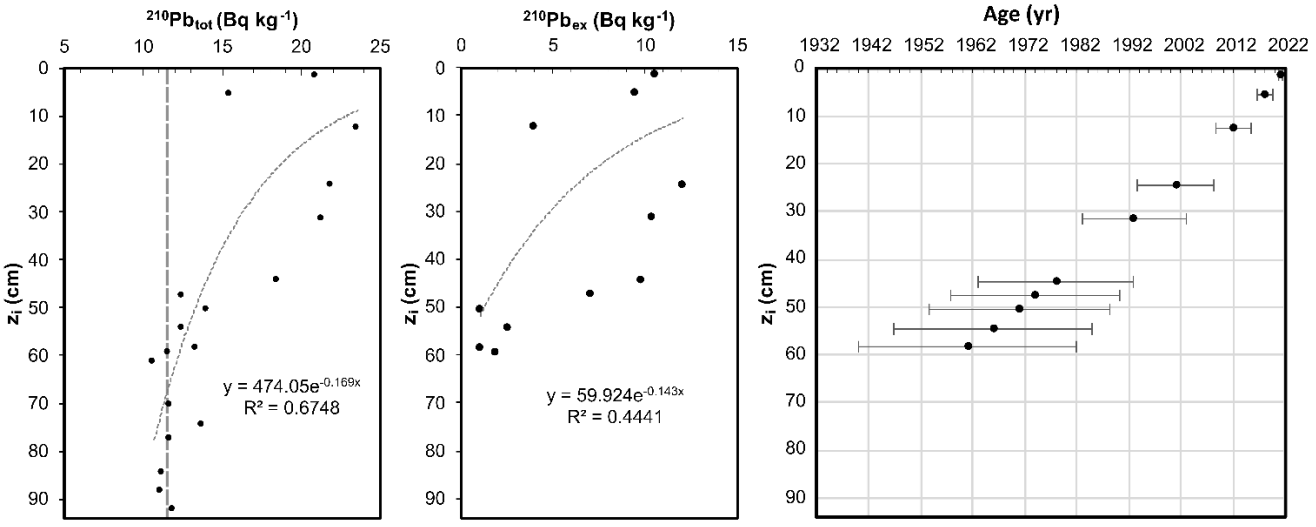

Figure 5. Dating results for core A1. To the left, total ^{210}Pb activities are shown relative to depth (on a dry weight basis); the loosely dashed line represents the supported ^{210}Pb (11.5 Bq kg^{-1}). In the middle, calculated excess ^{210}Pb is shown relative to depth. To the right, radiometric chronologies along the core relative to depth.

1.4.2 Microplastic content

Before presenting the concentration of MPs found along the core, it is important to depict the polymer types that the used methodology allowed to be detected; both the density of the solution used for separation of the MPs and the wavelength of the incident light are determinant (Table 3). Consequently, the detection of MPs in the present work is restricted to

EPS, PP, LDPE, weathered HDPE, and virgin PE. Other common plastic types, such as PS, PET, or PA, were either not counted, or its detection is uncertain.

Table 3. Detected MPs according to used solution for density separation, and light wavelength. Data taken from Ding & Ying (2015), Frias et al. (2018), Lakatos & Kalmár (2013), Patel (2016), Prata et al., (2019b). Some of the polymers lack fluorescence information under 365 nm light and are therefore labeled as "NI".

Polymer type	NaCl separated	Fluorescent under 365 nm	Detected MPs
Polystyrene (PS)	✓	×	×
Expanded polystyrene (EPS)	✓	✓	✓
Polypropylene (PP)	✓	✓	✓
Low-density polyethylene (LDPE)	✓	✓	✓
High-density polyethylene (HPDE)	✓	Only weathered	Only weathered
Polyethylene (PE)	✓	Only virgin	Only virgin
Ethylene vinyl acetate (EVA)	✓	NI	NI
Polyamide (PA)	✓	NI	NI
Nylon 6,6 (PA 6,6)	✓	Not specified	NI
Poly methyl methacrylate (PMMA)	✓	NI	NI
Polycarbonate (PC)	×	NI	×
Polyurethane (PU)	×	NI	×
Polyethylene terephthalate (PET)	×	✓	×
Polyvinyl chloride (PVC)	×	×	×
Polytetrafluoroethylene (PTFE)	×	NI	×
Cellulose acetate (CA)	×	✓	×

The concentration of microplastics, given in Figure 6 correspond to the measured items/kg (d.w.) after subtracting the particles found in the blanks and averaging those of the duplicates, for detailed data see Table A1 and A3. It was assumed that MPs were uniformly distributed on each core slice. The highest concentrations were found in the most surficial 15 cm, reaching up to 5358 items/kg in the year 2021±0.31 (sample 1-2 cm). A general decreasing tendency was observed toward the older sediment layers.

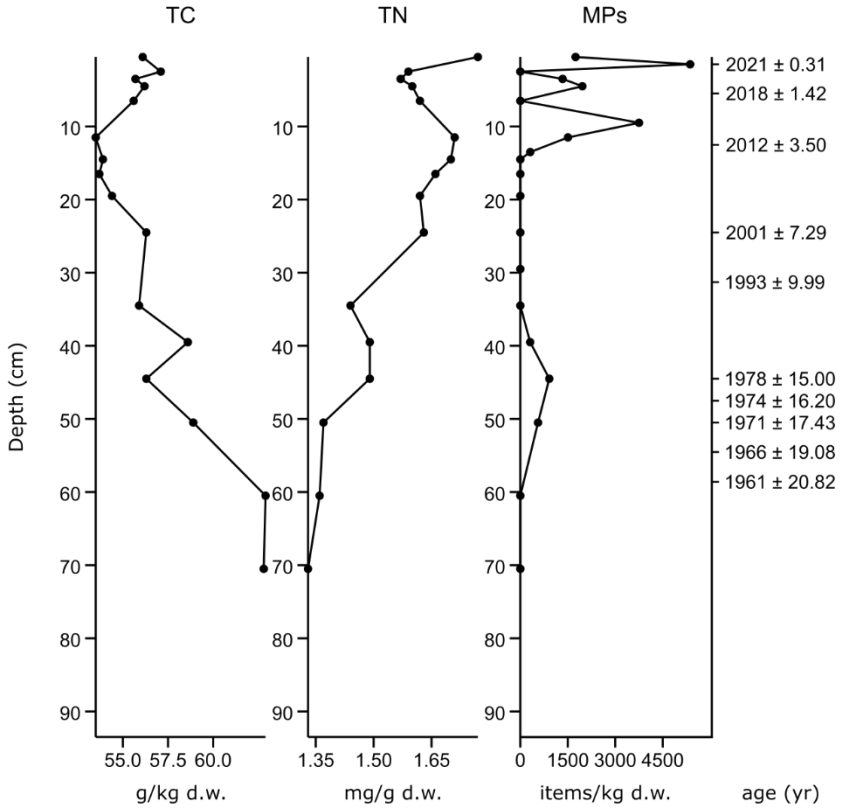

Figure 6. Analyses of total carbon (TC), total nitrogen (TN), and microplastic concentration (MPs) along the core A1 with calculated ages.

For the analyzed photos, the lower size detection limit of MPs ranged between 43.48-47.32 µm, with an average of 44.27 µm, and a standard deviation of 0.744 µm (given by the detection limit of MP-VAT 2.0A and MP-VAT 2.0, set at three pixels; Table A3). Sizes of the detected MPs ranged between 46-1013 µm (this range corresponds to the largest dimension of each particle, i.e., MaxFeret in Table A3), where 95% of them were smaller than 299 µm (Figure 7 and Table A3). These size values correspond to the total of detected particles minus a random subtraction of the corresponding procedural blanks (for each sample); this was made using the Excel functions “RAND”, “INDEX”, and “RANK”. No apparent size trend was observed along the core.

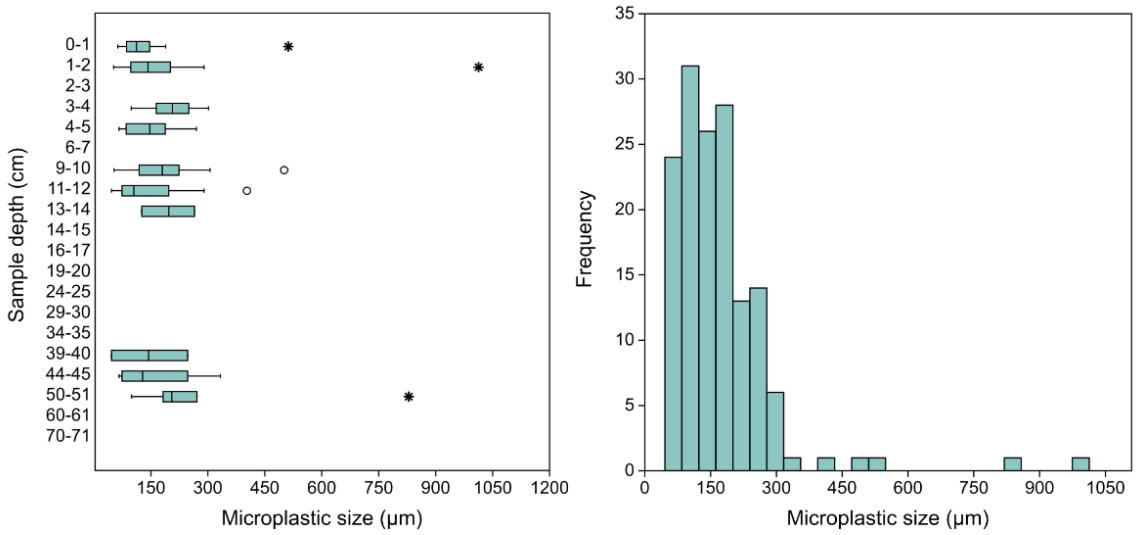

Figure 7. Box plot of microplastic size distribution along the core (left), where circles and stars represent mild and extreme outliers, respectively. Histogram for all detected particles (right).

Moreover, for the analyzed samples, MPs were mainly characterized as particles by MP-VAT 2.0A (Figure 8). The classification made by the macro includes three categories using circularity, which ranges between 0-1 for elongated and spherical MPs, respectively, i.e., fibers (0.0–0.3), fragments (0.3–0.6), and micro-spheres (0.6–1.0) following Prata et al. (2020a) and Prata et al. (2019b).

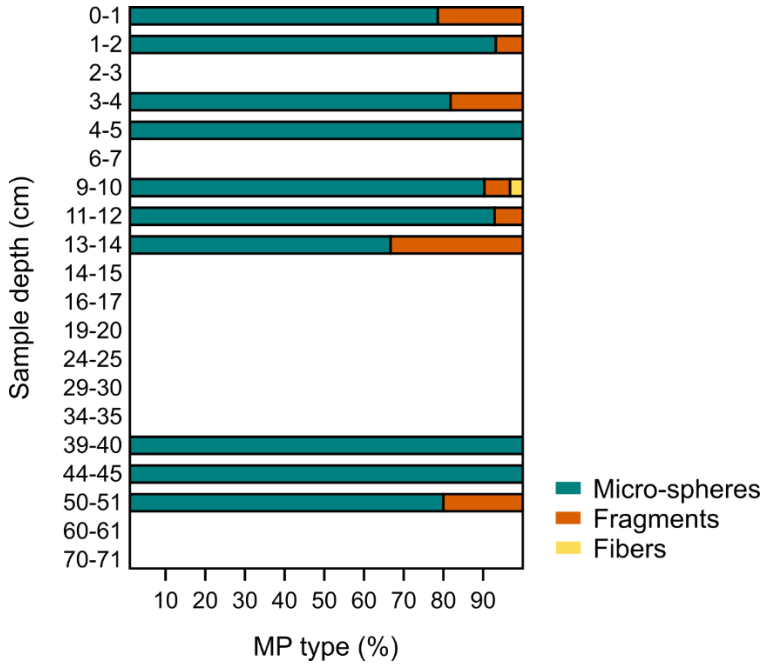

Figure 8. Microplastic type percentages for the studied samples. Micro-spheres, fragments and fibers from greatest to lowest circularity, respectively.

1.4.3 Geochemical analyses

As shown in Figure 6, a clear decreasing trend toward the surface was observed for TC measurements reaching the highest value at 60 cm depth (62.9 g/kg d.w.). Conversely, TN presented a clear increasing tendency toward the surface, reaching its highest value at 0 cm depth (1.77 mg/g d.w.).

1.5 Discussion

The *in situ* measurements taken at water surface at core sample location confirm the prevalence of marine conditions and indicate minimal influence of fresh water input (Table 1, Figure 2) as discussed by Parada Ruffinatti et al., (1996). In addition, as stated in the Study Area section, it is worth noting that apart from an apparent increase in surrounding vegetation (Figure 1), which mainly consists of mangrove, the morphology and dynamic of the lagoon have remained relatively constant throughout the years (Miranda & Parada Ruffinatti, 1987). A more detailed revision of changes in the morphology is presented in section 2.5 in the light of grain size results; however, since no MP size trend was observed, it is considered that the slight changes in water energy did not affect the deposition of this pollutant in the study area.

Regarding MP concentrations over time, a general increase of MPs was observed toward the most recent sediment layers, approximately, since 2010 (Figure 6). This has been reported in similar studies and has been interpreted to reflect the global increase in plastic consumption and production (Matsuguma et al., 2017; Turner et al., 2019; Yao et al., 2019). A more detailed view of the results (Figure 6) shows that the concentration of MPs did not exhibit a strictly exponential behavior; some variations in the surficial layers were observed. This might be attributed to a methodology bias since MPs might not have been uniformly distributed within the sediment slices. Moreover, it is worth noting that counts of zero MPs do not imply their absence, both because MPs smaller than 43.48-47.32 μm are likely to be present, and because not all polymer types were recovered by this methodology.

Additionally, the highest concentration was found for the year 2021±0.31 (5358 items/kg in sample 1-2 cm). Even though the COVID-19 world pandemic is known for the increased use of plastic both for biosafety and food packaging (Lee & Kim, 2022; Rusinque-Quintero et al., 2022), the time required for the transformation of these elements into secondary MPs may lead to a related peak further in the near future; moreover, primary MPs such as fibers,

associated with the increase in face mask use (Lee & Kim, 2022), were not found at that depth (Figure 8). Alternatively, the Iota hurricane in 2020 could have mobilized MPs from the Caribbean region that otherwise would not have reached the study area; this warrants additional studies.

Moreover, an anomalous presence of MPs was found for the year 1978±15.00 (around 45 cm) depth amidst a generalized apparent absence of them. Two possible explanations arise. On the one hand, hurricanes that crossed Colombian coasts might have remobilized large quantities of MP from the Caribbean. These might end up entering the lagoon due to marine currents when the normal input was too low to get registered. Such events were the Irene in 1971, Joan in 1988, Bret in 1993 (Ortíz Royero, 2007). However, the uncertainty of the age at these depths does not allow an accurate interpretation of these events as a source of MPs. On the other hand, methodological limitations might be responsible since the outer rim of each slice was not removed. According to IAEA (2021), pollutants from the surface might reach deeper sediment layers due to the movement of the pipe where the core is collected. Contamination during core slicing is possible as well.

To obtain a finer sediment chronology, analyses such as gamma spectrometry to accurately determine supported ^{210}Pb, and precise granulometry using methods such as laser diffraction are highly recommended and will allow further confirmation of the current age model. Moreover, higher resolution of measurements is required for a most reliable dating. It is also worth noting that the sedimentation rate calculated by Miranda & Parada Ruffinatti (1987) of 0.66 cm yr^{-1} differs the one obtained from the core dating model, 0.967 cm yr^{-1}. Such improvements to this age model are in course and will be available for future publications. Therefore, the current age results should be considered as preliminary and as a general reference. Moreover, future research should take the following into consideration:

- Historic plastic production, consumption, and recycling patterns in Colombia, particularly in Cartagena. For instance, the foundation of the organization Acoplásticos in 1961, which was created to associate and represent companies in the plastic production chain within the context of high demand of this product (Acoplásticos, n.d.); notably, in this decade several companies in the plastic industry emerged (Estrada Villareal, 2017). Moreover, the acquisition of Reficar SAS, an oil refinery, by Ecopetrol SA in 1974 marked a breaking point in consolidating the petrochemical industry of Cartagena; according to Acosta (2012), this represented an increase from 40,69% (1965) to 70,4% (1974) in the participation of the

petrochemical-plastic sector in the industry of Cartagena. Particularly, the development of this industry in the city is of relevance considering the predominance of primary MPs in the area (Acosta-Coley et al., 2019).

- A historical reconstruction of the potential sources of MPs in the region. As indicated by Galindo et al. (2023), the main sources of MPs in Colombian coastal areas include agriculture, population centers, industries, river inputs, tourism, wastewater, fishing, maritime activity, seaports and solid waste. A thorough analysis of changes in these sources over time is recommended along with detailed research on the economic activities.
- Polymer type analysis, which can support historical interpretation when linked to a detailed study of national production patterns of the various polymer types and their consumption and recycling. Fourier transform infrared spectroscopy (FTIR) and Raman spectroscopy are commonly used techniques for this purpose (Liu et al., 2022).
- The deposition of MPs in the sediment is not immediate, and primary and secondary MPs have different residence times in the water column, also influenced by polymer type (Hidalgo-Ruz et al., 2012). This means, for instance, that depending on the type of MP, a peak in consumption or production might not be immediately reflected in the sediment.
- A thorough analysis of storms should be performed considering both magnitude and distance from the study area.
- Both oceanographic and atmospheric models should be considered since marine and atmospheric currents play a significant role in MP transport and distribution (Acosta-Coley et al., 2019; UNEP, 2016; Yao et al., 2019). This can also be used to further confirm whether the influence of the Magdalena River is negligible as stated in Parada Ruffinatti et al. (1996).
- Since legislation on plastic has become more popular, it should be considered for historical analyses. For instance, Zheng et al. (2020) suggested a possible relationship between a slight recent decrease in MP abundance with a policy for plastic use reduction.

Regarding MP type, only small MPs were found in core A1 (95% smaller than 299 μm), which is related to the low water energy at the sampling point, where muddy sediments prevail (Section 2.4); bigger MPs are expected to be found closer to the entrance of the lagoon, where the water energy is higher. As shown in Figure 7, no trend was observed for MP size throughout the core.

Furthermore, it is not possible to accurately compare these results with other studies made in Colombia. Values of up to 2863 items/kg d.w. (Garcés-Ordóñez et al., 2019), and 2457 items/kg d.w. (Rangel-Buitrago, Arroyo-Olarte, et al., 2021) have been reported for sediments in the Caribbean coast; however, the smallest detected MPs were limited either by the use of 1 mm sieve, or by the visual capacity of detection of the investigator, respectively. In Acosta-Coley et al. (2019) a lower detection limit of 400 μm was used, but the results are reported in items/m^2. It is possible that a considerable number of MPs have remained overlooked due to the constraints imposed by detection limits. In turn, the adopted methodology enabled the measurement of MPs down to 44.27 μm thanks to the use of NR and image analysis, thereby recovering a broader range of MP sizes (Figure 7). Moreover, previous studies in Colombia have primarily focused on the sand surface in beach settings, down to 5 cm depth, making direct comparisons implausible.

In this spirit, the use of methodologies that allow a broad range of MP detection is recommended. For instance, to improve the one used in this study, employing separation solutions denser than NaCl, such as sodium tungstate dihydrate ($Na_2WO_4 \cdot 2H_2O$, 1.4 g/cm^3) or sodium iodide (NaI, 1.8 g/cm^3) (Frias et al., 2018) will allow recovering broader range of microplastic compositions (Table 3); furthermore, the use of 470 nm light, through NR-based techniques, is encouraged to enhance fluorescence (Prata et al., 2019b). In addition, the removal of the outer ring of sediment from the cores is advised to reduce error risk in counting procedures for pollution analyses (IAEA, 2021).

Previous studies show that secondary MPs are the most common in Colombian coasts, out of which PP and PE predominate (Galindo et al., 2023); in the area of Cartagena, almost all MPs in surface waters are represented by PE, PS, and PP, in decreasing abundance order (Garcés-Ordóñez et al., 2021). In the case of PE, the current method only allowed the counting of virgin particles (Table 3), which could imply an underestimation of a portion of the secondary MPs. However, Acosta-Coley et al. (2019) state that secondary MPs reach the highest concentrations in the vicinities of river mouths. The Magdalena River, which is the closest to Ciénaga de los Vásquez, has very low influence in this coastal lagoon (Parada Ruffinatti et al., 1996). Moreover, Acosta-Coley et al. (2019) found that Cartagena presents the highest relative contents of primary MPs for the Caribbean coast of Colombia. Consequently, the study area is thought be a reflection of this behavior, i.e., primary MPs might comprise a great portion of the detected particles; as shown in Figure 8, most detected particles correspond to micro-spheres,

which can be associated with micro-pellets and primary MPs. Accordingly, Turner et al. (2019) associated fiber contents to wastewater and airborne inputs; the prevalence of micro-spheres and fragments above fibers (Figure 8), could further indicate the limited influence of river input, with Cartagena being the main source of MPs.

1.5.1 Relationship with carbon and nitrogen

Regarding the effect of MPs in the sediment's chemistry, it was expected that the increase in this pollutant would cause an increase in carbon contents since this pollutant enters the system both as a carbon source for microorganisms and releases dissolved organic carbon increasing carbon storage (Ladewig et al., 2021; Rogers et al., 2020; Wang et al., 2022). However, TC measurements in the sediment presented a decreasing trend toward the surface; the highest values were found at 60 cm depth where MP concentration is zero (apparent absence) (Figure 6). This can be attributed to the rising content of inorganic carbon (bioclasts, like bivalve shells) toward the deeper sediment layers, as presented in section 2.4; a trend that could potentially create a masking effect on the impact of microplastics on carbon levels. The Pearson correlation between these variables was not significant: -0.23 (α=0.05, p=0.39, n=16). Consequently, separate organic and inorganic carbon analyses are highly recommended for this area.

Meanwhile, according to Miranda & Parada Ruffinatti (1987) nitrogen concentration is highly correlated to OM in Ciénaga de los Vásquez, suggesting a potential increase in nitrogen measurements with increasing MPs content; moreover, Hope et al. (2020) found increased nitrogen storage in the sediment in the presence of MPs. The concentration of TN did show a clear increasing trend toward the surficial sediment layers, as MPs did. Such an increase in TN over time might represent either a greater input of nitrogen (increase in production rates, accumulation of OM, an increase in nitrogen fixation, a decrease in water energy), or diminished denitrification (Libes, 2009; Wang et al., 2022). At around 45 cm depth, both variables (MPs and TN) presented a slight increase. However, where null concentrations of MPs occurred, TN contents presented variations (Figure 6). The Pearson correlation was not significant for these two variables: 0.35 (α=0.05, p=0.19, n=16).

Nevertheless, the influence of MPs on the nitrogen in marine sediments is rather complex and not yet fully understood; nitrogen fixation, storage, and denitrification are dependent not only of MP content, but also of MP polymer type; some polymers inhibit these processes, while

others promote them (Hope et al., 2020; Seeley et al., 2020; Wang et al., 2022). Moreover, the influence of MPs in the nitrogen cycle can be exerted before their burial since they can both affect microbial communities in the water column and the sinking rate of fecal pellets (Wang et al., 2022). Since TN measures all nitrogen species (NH_4^+, NO_2^-, NO_3^-, and organic nitrogen) as a whole, more detailed analyses could help us understand the historical effects in the sedimentary record. Consequently, the influence on Ciénaga de los Vásquez cannot be yet discarded; further studies should be conducted to reach a more conclusive determination. For a more detailed statistical analysis, refer to Section 3.

1.6 Conclusions

This study evaluated the temporal variations in microplastic (MP) concentrations in a sediment core from Ciénaga de los Vásquez, Cartagena, Colombia. The general increasing tendency toward the surface was consistent with several studies around the world reflecting the historical increase in plastic production, consumption, and pollution. In addition, the automated count of these particles using Nile Red and ImageJ allowed for a cheap and time-efficient assessment of historical MP concentrations, of MP sizes down to 44.27 μm. This method had not been used in similar studies in Colombia; therefore, akin broad-spectrum methodologies are highly advised both to enhance MP recovery and to allow comparison of the results across different studies. Moreover, since micro-spheres were dominant along the core, and the Magdalena River has negligible influence in the study area, primary MPs may constitute a significant portion of the MPs, where Cartagena is presumably the main source or MP pollution. In addition, despite the results showed no significant relationship between MP concentration and total carbon and nitrogen in the sediment, the influence of MPs on these elements cannot be ruled out and should be further studied. It is recommended to measure separately organic and inorganic carbon, and nitrogen species to best understand the historical effects of MPs on the carbon cycle and nitrogen fixation and denitrification processes. In sum, the use of the sediment core was of great utility to evaluate this pollutant from a temporal perspective and is highly suggested for future studies in various coastal settings from Colombia since it provides insights on its deposition and influence on the environment.

2. Changes in the community of benthic foraminifera over time

2.1 Abstract

The present study evaluated the community of benthic foraminifera within a sediment core from Ciénaga de los Vásquez, an open marine lagoon in Cartagena, Colombia. Over time, this lagoon has maintained its morphology and has shown no significant influence from the Magdalena River. This study aims to study the historical changes of the benthic foraminifera community, to reconstruct the environmental changes in the study area. Accordingly, total abundance, the relative abundance of the genus *Ammonia*, the *Ammonia-Elphidium* index, and test morphology indicated that the sediment of this lagoon has undergone an increase in organic matter and a decrease in water energy, which can be related to the both the narrowing of the central part of the lagoon and the growth of surrounding vegetation. However, the rapid increase in total abundance observed at around 20 cm depth coupled with a decrease in diversity might indicate the entrance of a stressor agent; therefore, taxonomic identification to species level, some detailed indexes, and identification of deformed tests are suggested to further evaluate the historical changes and pollution in the area.

2.2 Introduction

Foraminifera is a phylum of eukaryotic single-celled organisms belonging to the supergroup Rhizaria and the clade SAR (Saraswati, 2021). These organisms construct an outer shell called *test*, which can be composed of calcium carbonate, aggregate particles or, less commonly, organic material (Haynes, 1981). Inorganic tests have provided over the years a significant amount of information about their environment due to their good preservation in the sediments and in sedimentary rocks (Jones, 2014).

These organisms first appeared in the Cambrian Period and have become the most diverse group of shelled microorganisms in contemporary oceans (Sen Gupta, 2013). Planktonic and

benthic foraminifera inhabit the oceans' water column and bottoms, respectively, but benthic foraminifera are both the most diverse and most abundant in coastal settings (Jones, 2014). The distribution of benthic foraminifera is linked to environmental factors such as temperature, salinity, pH, depth, and substrate characteristics (Acosta-Herrera, 2004; Murray, 2006).

Coastal environments are particularly interesting for studying foraminifera as they are more directly exposed to anthropogenic-related stressors. Therefore, the present study aimed to determine changes in the community of benthic foraminifera to gain insights on environmental changes over time. The selected study area was Ciénaga de los Vásquez, an open marine lagoon in Cartagena, Colombia, which is relatively isolated from tourism, has negligible freshwater input (Parada Ruffinatti et al., 1996), and previous studies, both in surficial sediment and sediment cores, were conducted within the lagoon, providing a reference point (Miranda & Parada Ruffinatti, 1987; Parada Ruffinatti et al., 1996). During the regional dry season in April 2022, a sediment core was collected from this lagoon. Subsequently, an analysis of the benthic foraminifera community was performed, to examine changes over time.

2.3 Methods

As described in Section 1.3, two cores were collected, from which core A2 was used to analyze foraminifera in the study area. For each analyzed sample, grain size fractions were obtained by sieving, and foraminifera were analyzed for >125 μm fractions. The analyzed samples are shown in Table 4.

Regarding grain size analysis, the methodology implemented and validated in the LABCAM was followed with some variations. A small aliquot of wet sediment (between 1.2 and 5.8 g according to sample wet weight %) was oven-dried at 104 °C for 24 h, while the rest of the sample was gently rinsed with tap water through a 63 μm sieve and oven-dried at 50 °C (instead of 104 °C, to prevent affecting future geochemical analysis on foraminifera tests). Bivalves bigger than 2 cm were removed from the samples before drying. The dried sample was then weighed and allowed to react with 10% H_2O_2 (Feldmeijer et al., 2013) until no further reaction was observed. This step prevented particle agglomeration caused by OM content (which results in an inaccurate grain size distribution). After rinsing the samples to remove any remaining mud (using a 63 μm sieve), they were oven-dried and sieved using a mechanical sieve-shaker for 15 minutes with sieve sizes of 125, 250, 500, 1000, and 2000 μm. Each fraction

was weighted and stored in labeled plastic vials. The dry aliquot was used to calculate the mud fraction for the entire sample.

It is worth noting that the aforementioned protocol is typically recommended for sediment samples weighing around 250-400 g w.w.. However, the analyzed samples had a reduced weight ranging between 57-98 g w.w.. This variation in sample size may have introduced some level of inaccuracy in the analysis; however, the protocol was diligently followed to the best extent possible, resulting in a reasonably estimated grain size distribution within the study's limitations.

Table 4. Analysis per sample in core A2. Forams is used as an abbreviation of foraminifera.

Depth	Dried	Grain size	Forams	Depth	Dried	Grain size	Forams
0-1	X	X	X	44-45	X	X	X
1-2	X	X	X	45-46			
2-3	X	X	X	46-47			
3-4	X	X	X	47-48			
4-5	X	X	X	48-49			
5-6	X	X		49-50			
6-7	X	X	X	50-51	X	X	X
7-8	X	X		51-52			
8-9	X	X	X	52-53			
9-10	X	X	X	53-54			
10-11	X	X		54-55			
11-12	X	X	X	55-56			
12-13	X	X		56-57			
13-14	X	X	X	57-58			
14-15	X	X	X	58-59			
15-16	X	X		59-60			
16-17	X	X	X	60-61	X	X	X
17-18	X	X		61-62			
18-19	X	X		62-63			
19-20	X	X	X	63-64			
20-21				64-65			
21-22	X	X		65-66			
22-23				66-67			
23-24				67-68			
24-25	X	X	X	68-69			
25-26				69-70			
26-27				70-71	X	X	X
27-28				71-72			
28-29				72-73			
29-30	X	X	X	73-74			
30-31				74-75			
31-32				75-76			
32-33				76-77			
33-34				77-78			
34-35	X	X	X	78-79			
35-36				79-80			

Depth	Dried	Grain size	Forams	Depth	Dried	Grain size	Forams
36-37				80-81			
37-38				81-82			
38-39				82-83			
39-40	X	X	X	83-84			
40-41				84-85			
41-42				85-86			
42-43				86-87			
43-44				87-88			

For the foraminifera analysis, a proportional subsample of sediment was taken from each fraction (>125 μm) to ensure adequate representation. This means, for instance, that 1/16 of each size fraction was extracted from a given sample using an analytic balance (with precision of 0,001 g). All size fractions, collectively, constituted a subsample, for which the weight was registered. The size of the subsamples varied throughout the core due to changes in total abundance; it was ensured that each subsample contained 250-300 individuals to attain a statistically representative analysis (Murray, 2006). Each subsample was fully picked, and foraminifera were mounted on microfossil slides obtaining the total assemblage.

Individuals were sorted under at up to 60× magnification with a stereomicroscope (Leica S6E). Abundance of benthic foraminifera (tests per gram of dry sediment) and their relative abundances for wall type, genus *Ammonia* Brünnich, 1771, family Elphidiiae Galloway, 1933, and twelve test morphologies (see section 2.4) were calculated.

2.4 Results

The core A2 consisted mostly of muddy sediment, with mud content ranging from 83.4% to 97.7% (Figure 9). In the sediment fractions above 63 μm, the dominant particles were very fine and fine sand which increased toward the surface as well; conversely, medium, coarse, very coarse sand, and granules decreased in abundance toward the surface. Additionally, the sediment fractions above 63 μm were mostly composed of bioclasts, these consisted of fragments of corals, calcareous algae, echinoderms, polychaeta, gastropods, and bivalves; scarce quartz grains were found, all of them presented low sphericity and angular shapes (Figure 10). All grains in the coarsest fractions consisted of bioclasts. Botanical-derived OM residues were found to increase in abundance toward the surficial samples, where their digestion with H_2O_2 accounted for a reduction of up to 18% in dry weight. Abundant ostracods were found as well.

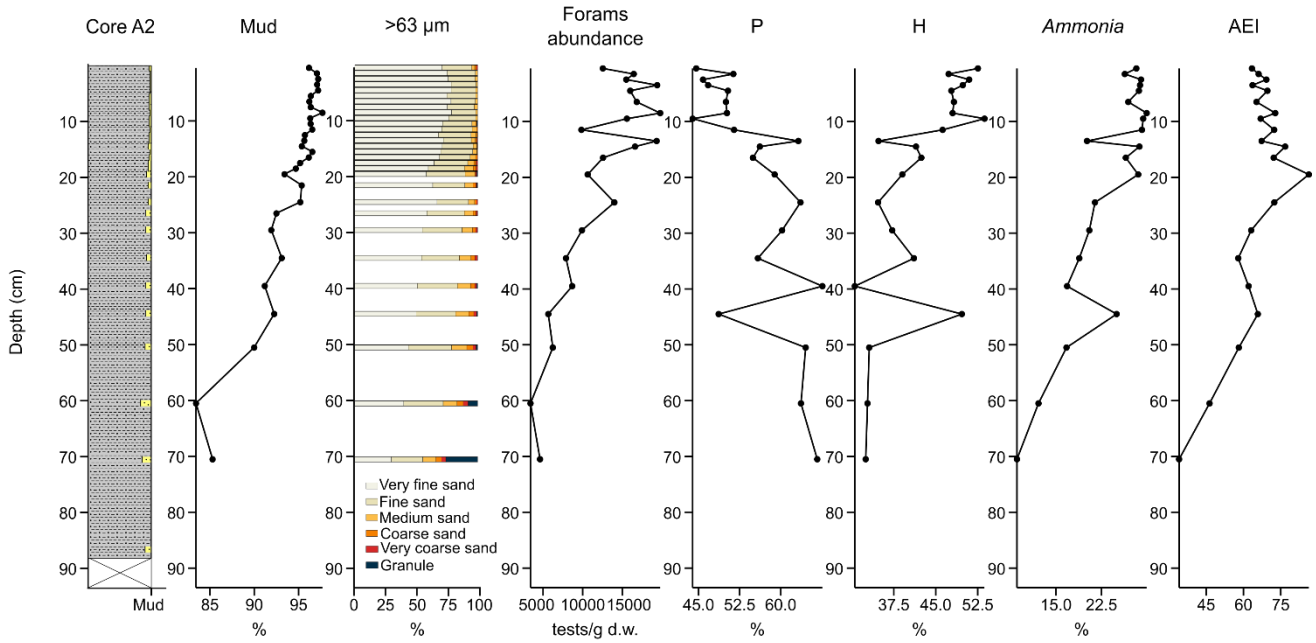

Figure 9. Grain size along core A2, benthic foraminifera abundance per gram of dry sediment, porcelaneous (P) and hyaline (H) wall test relative abundances, *Ammonia* relative abundance, and *Ammonia-Elphidium* index (AEI).

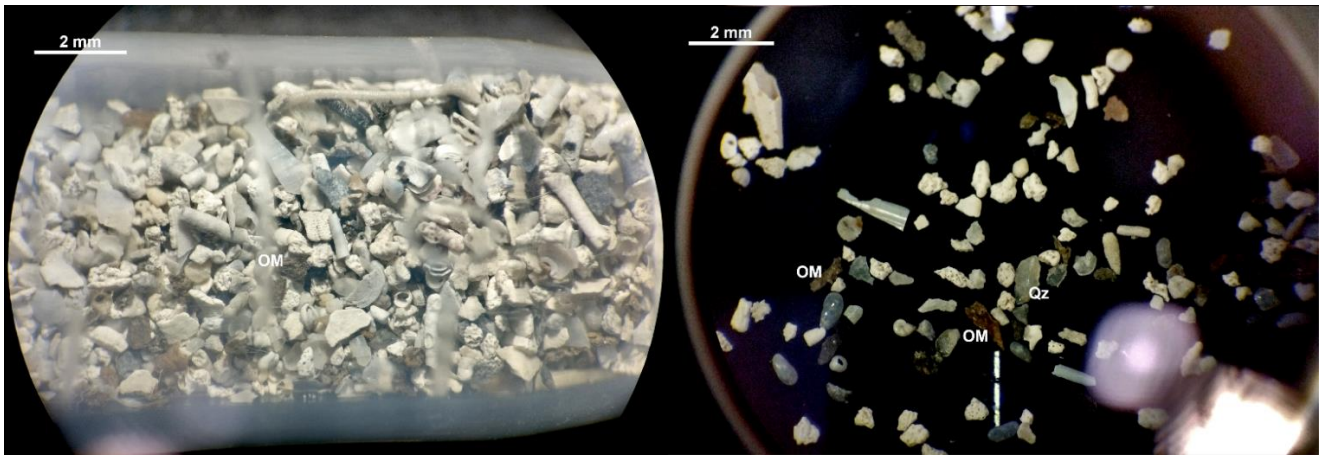

Figure 10. General view of the sediment fractions above 63 µm. The photo on the left shows sample 19-20 within a plastic vial, and the photo on the right shows sample 60-61 on the picking tray. The prevalence of bioclasts is visible in both photographs. Some organic matter (OM) fragments are visible, and an angular quartz grain is shown (Qz).

A general increasing trend in benthic foraminifera abundance was observed toward the most surficial samples (Figure 9). Planktonic foraminifera were also found; however, all data presented in this study were calculated for the benthic individuals. In the total assemblage, planktonic foraminifera were very scarce accounting for 0.0 to 1.13 % with an average of 0.44 %.

The tests per gram of dry sediment (tests/g d.w.) at around 10 cm depth were approximately three times those at around 60 cm depth (reaching up to 19,785 tests/g). The most abundant test walls were porcelaneous and hyaline, which were inversely correlated and have remained relatively constant during the deposition of the most recent 10 cm of sediment (Figure 9); agglutinated tests accounted for between 0.85 and 3.5 % of all benthic tests, with an average of 2.27 %. Such test wall type configuration allowed categorizing Ciénaga de los Vásquez in the domains of normal marine lagoon to hypersaline lagoon (Figure 11).

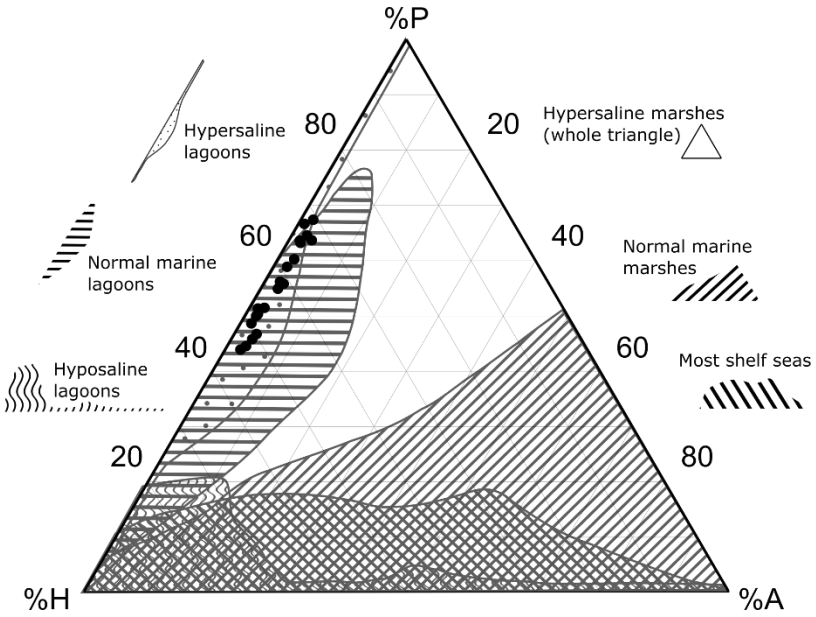

Figure 11. Test wall type ternary plot depicting marine environment setting and core A2 samples. %P refers to porcelaneous, %H to hyaline, and %A to agglutinated tests. Adapted from J. W. Murray (1991).

The relative abundance of *Ammonia* increased toward the surficial samples, mirroring the pattern observed for hyaline tests, where this genus was the most prevalent among this test type. Relatively constant abundances were observed for the most surficial 20 cm. Figure 12 presents photographs of some of the individuals of this genus; some tests were filled with pyrite, which was oxidized by the H_2O_2 treatment.

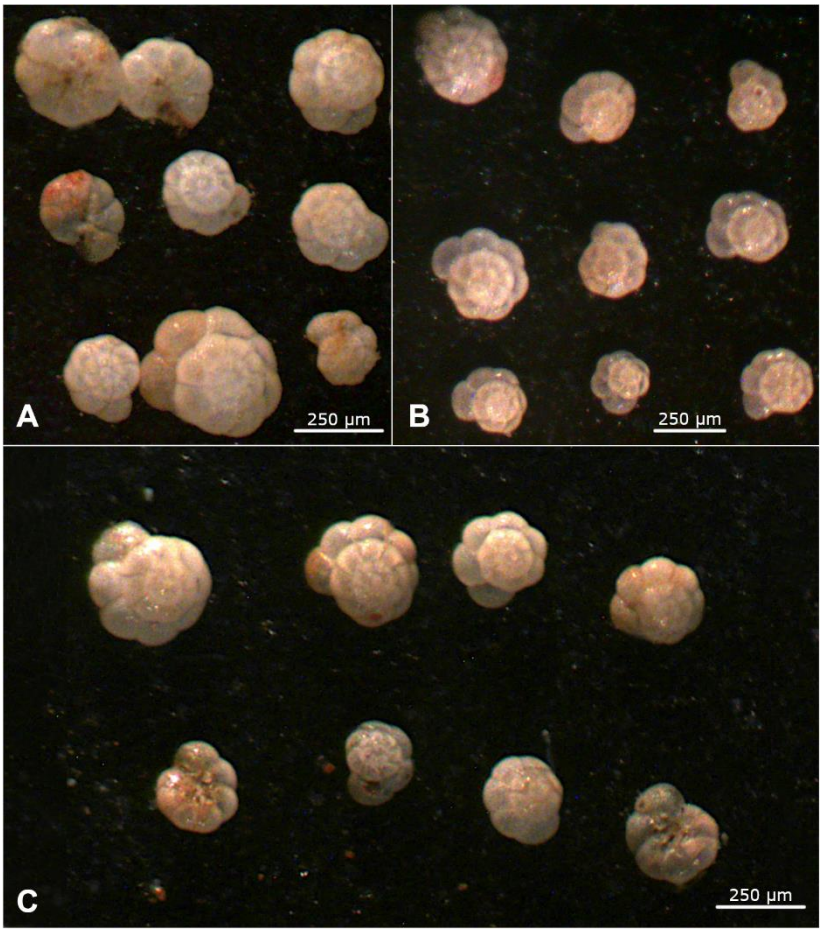

Figure 12. Representative individuals of the genus *Ammonia* from samples 3-4 (A), 19-20 (B), and 14-15 (C).

The relative abundances of the family Elphidiiae were determined to calculate the *Ammonia-Elphidium* index (AEI), as follows:

$$AEI = \frac{N_A}{N_A + N_E} * 100,$$

where N_A refers to the numbers of *Ammonia,* and N_E refers to those of *Elphidium* and *Cribroelphidium* after Alves Martins et al., (2020) and Carnahan et al., (2009), i.e., the family Elphidiiae (Figure 13). These authors include both genera in the *Elphidium* category both because of uncertainties in the taxonomy of this group, and because both genera have similar environmental sensitivities.

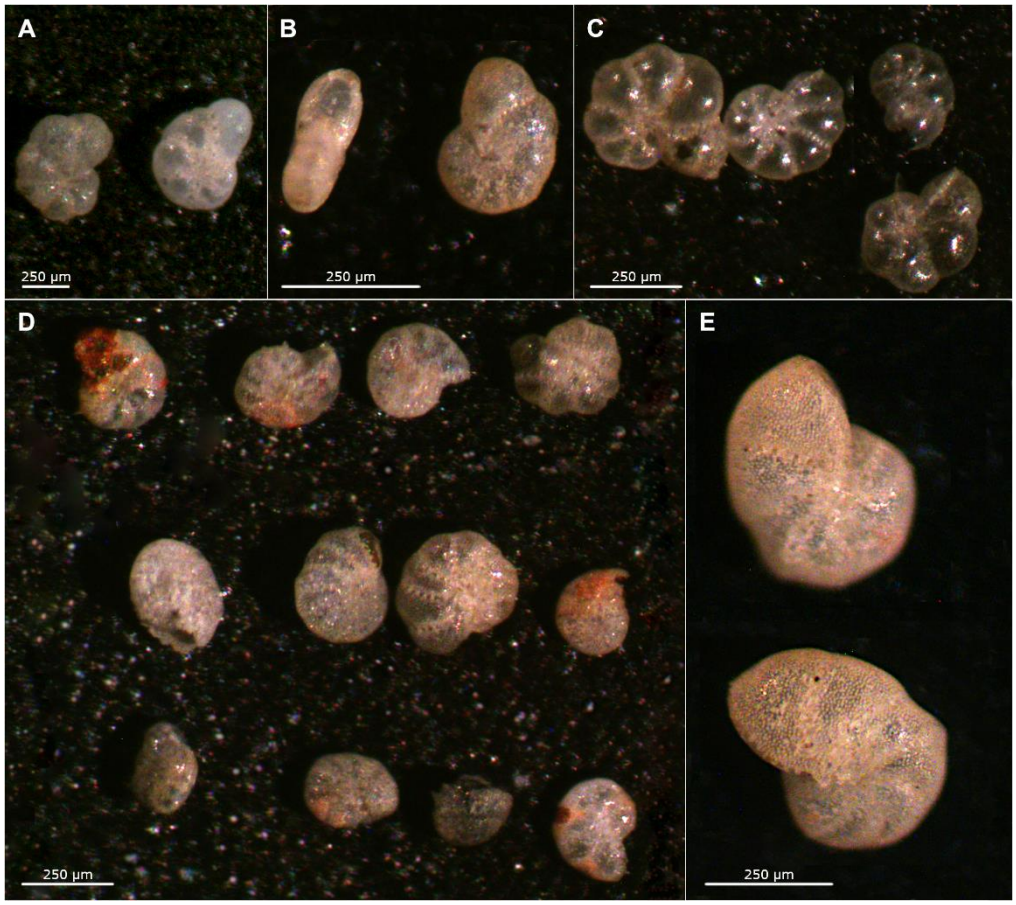

Figure 13. Representative individuals of the family Elphidiiae. Photographs from samples 11-12 (A), 34-35 (B), 50-51 (C), 50-51 (D), and 70-71 (E).

The AEI presented a generalized increasing tendency throughout the core, stabilizing in the most recent 20 cm sediment samples with a slight downward trend (Figure 9). The AEI is a qualitative indicator of oxygenated conditions for 0% values, and dysoxic-anoxic conditions for 100% values (Alves Martins et al., 2020). Consequently, a generalized decrease in oxygen levels of the sediment can be deduced, with a slight and steady increase in the most recent layers.

In addition, a classification of test morphology was made according to chamber arrangement and coiling types, following the descriptions of Acosta-Herrera (2004) and Rönnfeld (2008), which resulted in twelve categories hereafter referred to as M1, M2,..., M12 (Figure 14):

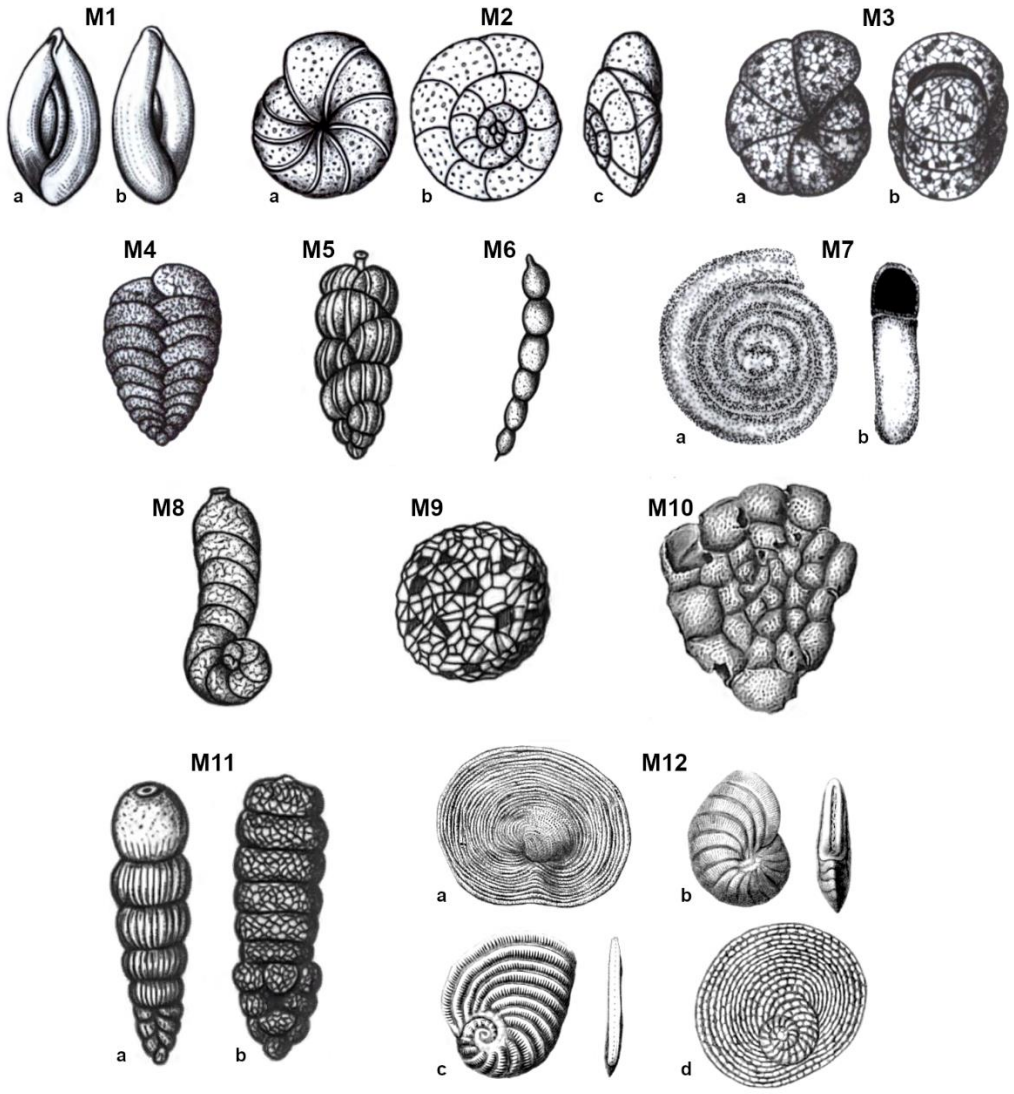

Figure 14. Test morphology categories according to chamber arrangement and coiling types. M1 a, b: miliolid coiling; M2 a, b, c: trochospiral coiling in ventral, spiral, and edge views, respectively; M3 a, b: planispiral involute coiling in lateral and edge views, respectively; M4: biserial test; M5: triserial test; M6: uniserial test; M7a, b: planispiral evolute coiling in lateral and edge views, respectively; M8: spiral to serial test; M9: single chambered test; M10: cyclic annular-discoidal test; M11 a, b: bi- tri- to uniserial test; and M12 a, b, c, d: most common tests of the superfamily Soritoidea Ehrenberg, 1839 (Illustrations from Acosta-Herrera, 2004; Nares et al., 1884; WoRMS: https://www.marinespecies.org)

A specific category was assigned to tests belonging to the Soritoidea superfamily (M12); this was because some of the tests could not be allocated to only one of the other categories, and because of their shared environmental requirements (Murray, 2006). Figure 15 presents the relative abundances of each test form along the core. M1, M2, M3, M4 and M12, listed in descending order of abundance, were the most prevalent among the twelve categories, i.e., miliolid, trochospiral, planispiral involute, biserial, and tests of the Soritoidea superfamily.

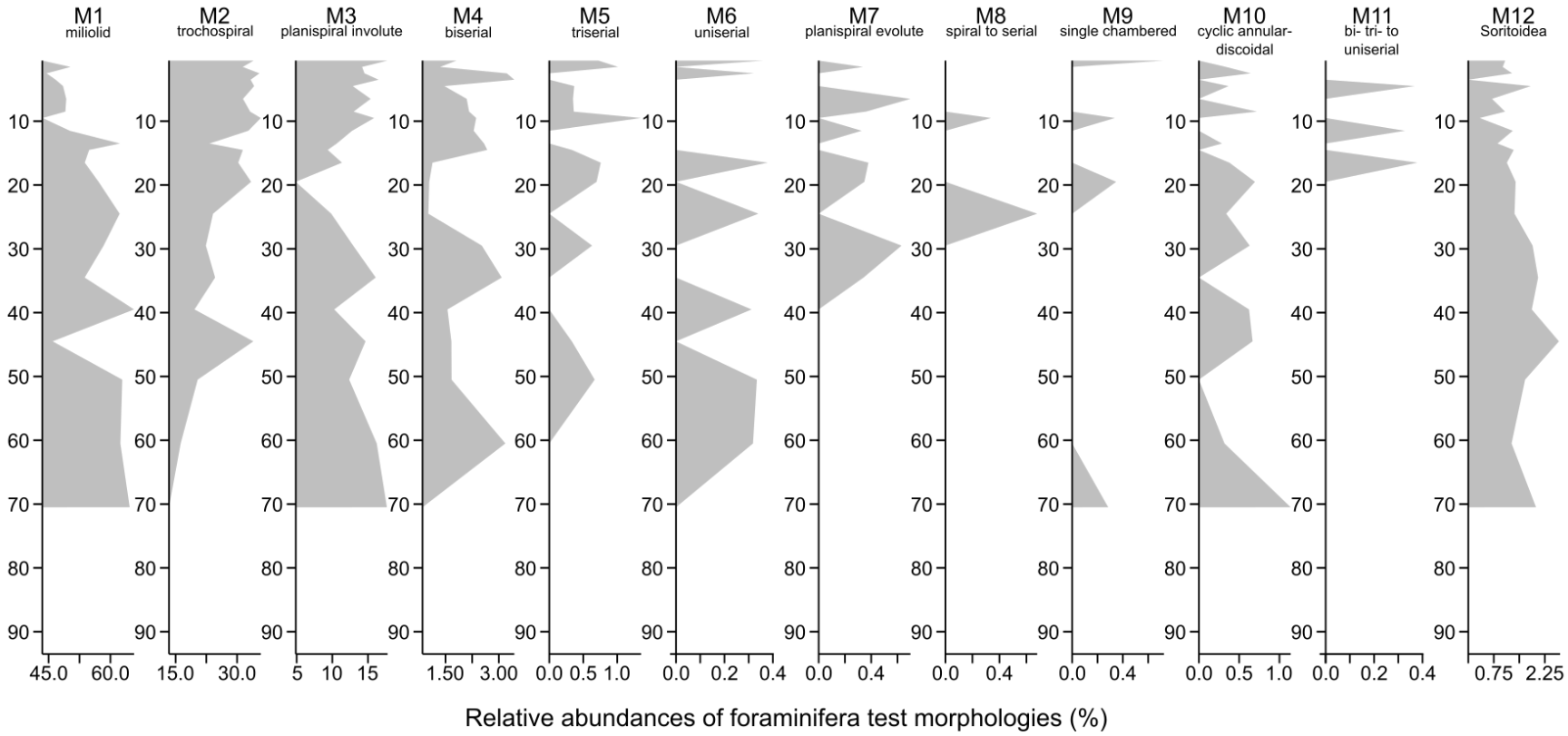

Figure 15. Relative abundances of benthic foraminifera test morphologies. M1 corresponds to morphology 1 of Figure 14, and subsequent morphologies (M2 to M12) correspond to the respective shapes in the same order. The deepest analyzed sample corresponds to 70-71 cm depth.

Most morphologies presented strong variations of abundance with no clear tendency along the core. Conversely, M1 and M2 presented a decreasing and increasing tendency toward the surface, respectively.

It is worth noting that a peak was presented at around 45 cm depth for some of the studied variables: hyaline and porcelaneous test wall types, *Ammonia* relative abundance, AEI, and morphologies M1, M2, M3, M5, M6, M10, and M12. Refer to Table A4 for all detailed results of benthic foraminifera, and to Appendix C for a plate showing photographs of an example individual for each morphology.

2.5 Discussion

The morphology of Ciénaga de los Vásquez appears to have remained stable over the past decades, with no significant changes (Figure 1). Nevertheless, upon closer examination of the central narrowing, it is visible that sediment has deposited in that area restricting water flow between the outer and the inner parts of the lagoon. This reduction in space can explain the observed reduction in grain size (Figure 9), as it restrains the water energy reaching the inner part.

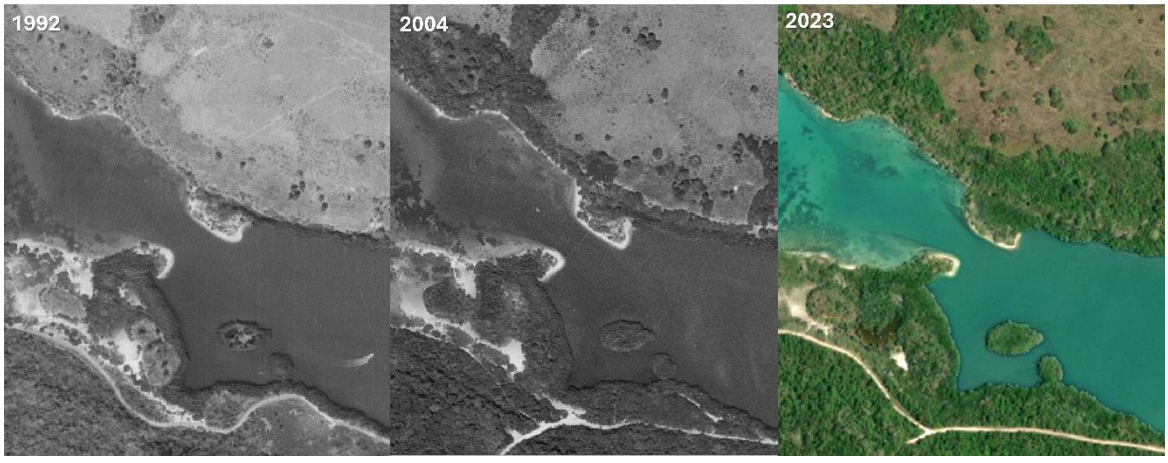

Figure 16. Close view of the central narrowing of Ciénaga de los Vásquez. The space for water flow to the inner part of the lagoon has reduced in the last years.

According to the analyzed sediment, the lack of influence from Canal del Dique discharges has been a consistent feature, as evidenced by the angular shape, low sphericity and scarcity of quartz grains, which was already observed in this lagoon by Parada Ruffinatti et al. (1996). However, the community of benthic foraminifera presented some variations.

A general increase in total foraminifera abundance was observed (Figure 9). This may be attributed to either an increased supply in OM (Klootwijk et al., 2021), or to the decrease in grain size (Pearson's correlation of 0.84, α=0.05, p=1.9e^{-6}). However, a rapid increase in total abundance was observed toward the surface, at 20 cm depth, which was not visible in the grain size and might be an indicator of a stressed environment (Suokhrie & Saraswat, 2017). Consequently, further analysis on the diversity of the community is advised since its reduction along with such a rapid increase in total abundance could indicate environmental changes such as pollution in the area (See section 3). According to Parada Ruffinatti et al. (1996), the normal behavior of foraminifera diversity in Ciénaga de los Vásquez is to increase with increasing OM inputs; therefore, a decrease in diversity along with an increase in OM would be atypical and warrant further study. Recognition of deformed tests, can also be a tool in further studies to identify pollution in the area (Suokhrie & Saraswat, 2017).

The genus *Ammonia* was set apart within the assemblage for its strong correlation to sediment conditions in the area (Miranda & Parada Ruffinatti, 1987). As stated by these authors, this genus was most common in Ciénaga de los Vásquez where the highest contents of mud occurred; Murray (2005) stated that *Ammonia* is most common where mud content surpasses 80% in the sediment. In addition this genus has been recognized to proliferate under environmental stress settings and high OM conditions (Hallock, 2012; Losada Muñoz & Parada Ruffinatti, 1986; Miranda & Parada Ruffinatti, 1987; Murray, 2006). An apparent increase in the surrounding vegetation (Figure 1) can be associated with increasing OM supply in the lagoon, which was observed during sediment treatment as indicated in section 2.4.
Such increasing tendency of *Ammonia* was already observed in sediment core analyses by Parada Ruffinatti et al. (1996) on this lagoon. Moreover, these authors also identified a decrease in the relative abundance of miliolid individuals (genera *Quinqueloculina* and *Triloculina*) toward the surface. In the present study, those genera were represented by M1; notably, such a decrease was one of the current findings (Figure 9 and Figure 15), and according to those authors, these changes indicate a continuous diminution in the water energy of the lagoon as well.

It is noteworthy that the relative abundances of *Ammonia beccarii* of Miranda & Parada Ruffinatti (1987) are equivalent to those presented here as the genus *Ammonia*. The taxonomy of this genus has been controversial over the years. Miranda & Parada Ruffinatti (1987) only

reported two variants for *Ammonia* for the same species in this lagoon, i.e., *Ammonia beccarii* var *tepida* and *Ammonia beccarii* var *sobrina*. Afterwards, Parada Ruffinatti (1992) stated that *Ammonia beccarii* is a cosmopolitan species that presents several ecophenotypic variations that should not be used as different species as some authors did. However, in the past decades, molecular genetics has proven that such ecophenotypic variations are in fact different species, and *Ammonia beccarii* should not be used as a group term (Murray, 2006). In fact, molecular sequencing has led to the recognition of up to 67 *Ammonia* species, whose global distribution and morphology are comprehensively presented by Hayward et al. (2021). Therefore, the identification of *Ammonia*, as a genus, allows direct comparison with previous works in the study area.

In addition, the AEI provides insights about the oxygenation levels in coastal regions since *Ammonia* and *Elphidium* are the most common genera in shallow waters, and the former genus is more resistant to low oxygen conditions than the latter (Hayward et al., 2021; Pregnolato et al., 2018). This index indicated that oxygenation levels decreased since the time of deposition of the deepest sediment layers, reaching its lowest level at 20 cm depth. Subsequently, a recovery in sediment oxygenation was indicated by a decrease in the index toward the surface (Figure 9). The general decrease in this index can be attributed to the increase in OM.

Moreover, the changes in foraminifera morphologies (Figure 15) might indicate variating conditions in the sediment over time, which have either favored or hindered the presence of each morphology. As stated before, the most abundant were M1 and M2, which presented, respectively, clear decreasing and increasing tendencies toward the surface. Since M1 is representative of miliolid genera and M2 is strongly correlated to *Ammonia* (Pearson correlation 0.97, α=0.05, $p=2.2e^{-13}$), the interpretation of these variations remains to be a continuous decrease in the water energy of the lagoon (Parada Ruffinatti et al., 1996). M12 also presented a generalized decreasing tendency toward the surface; this might indicate a reduction in oligotrophic conditions to which Soritoidea is generally associated (Jones, 2014; Sen Gupta, 2013). This is consistent with the decrease in water energy, as evidenced by the decrease in grain size (Nichols, 2009), and the increase in OM in the sediment. The decrease in water energy might be related to both the narrowing of the central part of the lagoon and the increased presence of mangroves in the area. Meanwhile, the other morphologies presented no clear trend and should be complemented with species identification; in particular, abundances of M5 to M11 should be taken prudently since their relative abundances are lower

than 1% and are thus close to confidence limits (Murray, 2006). Finally, some of the findings in this study warrant further analyses, as their causes may be linked to recent anthropogenic pressures. For instance, the observed change in tendency at around 20 cm depth for foraminifera abundance, *Ammonia* and AEI (Figure 9) might indicate the entry of a stressor in the lagoon. This result, among those previously exposed, are discussed in Section 3 along with total carbon, total nitrogen, and microplastic analyses in the study area.

Future identification to species level and identification of deformed tests are highly encouraged to best understand foraminiferal associations over time and their response to environmental variables. In this spirit, species identification will also allow more detailed indexes to be calculated. For instance, the results from the Enhanced Benthic Foraminifera Oxygen Index (EBFOI) could be compared with those of the AEI to gain a more comprehensive understanding of oxygenation in the sediment, and the Trophic Oxygen model (TROX) using epifaunal and infaunal species can improve the interpretations on OM (Kranner et al., 2022). Finally, it is recommended to further analyze miliolid and trochospiral individuals under the light of the Benthic Foraminiferal Salinity Index (BFS), since salinity might also contribute to the observed historical changes (Pérez-Asensio & Rodríguez-Ramírez, 2020).

2.6 Conclusions

The community of benthic foraminifera from Ciénaga de los Vásquez underwent some changes over time. A decrease in water energy was evidenced from grain size and was correlated to an increase in total abundance (reaching up to 19,785 tests/g), to an increase in the relative abundance of the genus *Ammonia*, and a decrease in that of miliolid individuals. A general increase in organic matter, possibly due to the growth of surrounding vegetation, was associated with these results. Moreover, a reduction of the relative abundance of Soritoidea was also associated to these conditions since this superfamily is related to oligotrophic conditions. In addition, the *Ammonia-Elphidium* index indicated a generalized decrease in sediment oxygenation, reaching its lowest point at 20 cm depth, followed by a slight recovery to the surface. Notably, at this depth, other variables, such as total abundance and *Ammonia* exhibited changes in their trends as well. It is recommended to identify the foraminifera at the species level since the observed rapid increase in abundance along with a decrease in diversity could indicate the entry of a pollutant into the area. The identification of deformed tests might also provide a tool to assess pollution in the area. Such detailed analyses, in conjunction with sediment chemistry and pollutants measurements, will contribute to a deeper understanding of how benthic foraminifera associations have responded to environmental changes over time.

3. Discussion

Considering the findings presented in chapters 1 and 2, the current discussion addresses the influence of MPs on the community of benthic foraminifera. As stated before, two cores were taken from the inner part of Ciénaga de los Vásquez, Cartagena, at 13.5 m from each other (Figure 2), which, for the present discussion are assumed to be correlatable. Both were taken within a small area where conditions such as grain size, and calcium carbonate, OM, and organic nitrogen contents are uniform according to Miranda & Parada Ruffinatti (1987). However, some recommendations are provided in section 4.2 to best ensure good correlation for analyzed cores in future studies.

As stated in the Introduction, the influence of MPs on benthic foraminifera has been assessed at cellular and individual levels (Birarda et al., 2021; Grefstad, 2019). Given the generalized small size of MPs in the study area, there is a propensity to interaction between foraminifera and these particles and ingestion of them is possible as well (Grefstad, 2019). In addition, the leachates produced by MPs might be causing cellular damage in some of the species (Birarda et al., 2021). Moreover, the increase in MP concentration in the sedimentary record has been found to correlate with an increase in MP particles in agglutinated foraminifera (Plafcan et al., 2024). Such effects may conduce to changes in the composition of the community (Bouchet et al., 2023), which is what the current discussion focuses on.

3.1 Statistical approach

As mentioned previously, benthic foraminifera respond to changes in their environment, which make them great tools for pollution assessment (Jones, 2014). To explore whether the community has been affected by MPs, two statistical approaches are presented next.

Initially, a Pearson's correlation matrix was made in RStudio (version 4.1.1) for all variables (at 95% confidence interval). The mode *pairwise.complete.obs* was used, which calculates the

correlation for each pair of variables using all complete pairs of observations on them (this mode was selected considering the absence of observations for several depths in certain variables). As shown in Figure 17, most variables that describe the community of benthic foraminifera present higher correlation values with granulometry (represented by mud content), TC, and TN, than with MPs concentration. As explained in section 1.5.1, no significant relationship was observed between MPs and the characteristics of the sediment expressed by TC and TN. The results seem to indicate that the community has responded most to changes in the sediment that can be attributed to an increase in OM and a decrease in water energy, as explained in section 2.5. However, triserial morphology (M5) did present higher correlation with MPs than with any of the other variables (0.61, α=0.05, p=0.005, n=20).

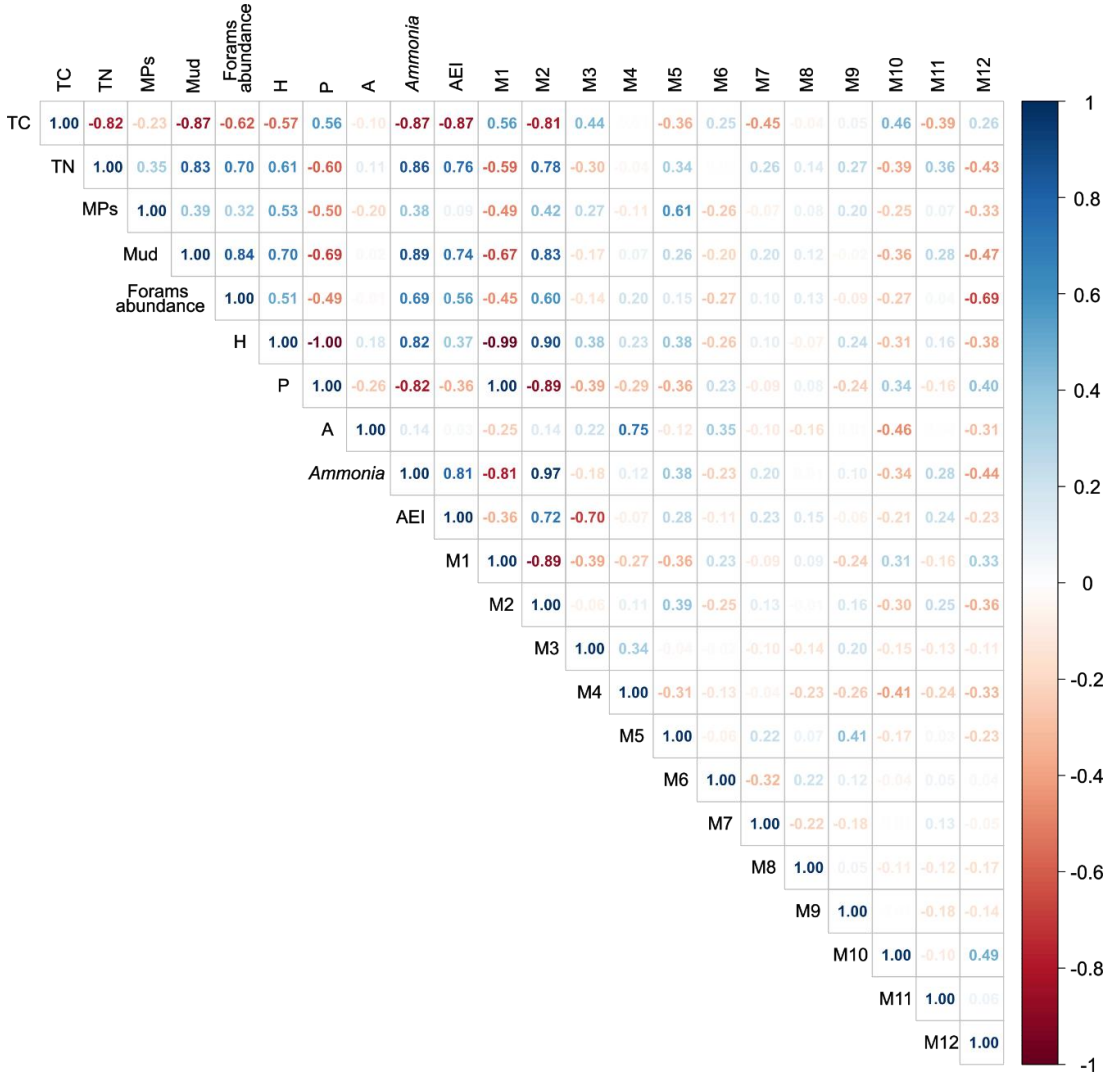

Figure 17. Pearson's correlation matrix for all biotic and abiotic variables. TC represents total carbon, TN is total nitrogen, and MPs is the concentration of microplastics. The relative abundances of mud,

hyaline (H), porcelaneous (P), agglutinated (A), the genus *Ammonia*, and morphologies (M1 to M12) are included. AEI is the *Ammonia-Elphidium* index. The color bar indicates the Pearson's correlation coefficient for each pair of variables.

For the second approach, the variable's matrix underwent a transformation. This was required since some statistical methods exhibit issues with missing data. At first, imputation was performed to obtain a matrix with no missing values.

It is recommended that imputed observations do not exceed 5% of the data; therefore, a subset of the data was extracted where 16 depths had no missing values, and 5 depths had only two to three missing values, which led to the need to impute 11 values (1.8% of the data). The RStudio library MICE (short for multivariate imputation by chained equations) was used. This method predicts missing values by using the actual observations from all other variables and incorporates an aleatory component set by a user-defined seed. The imputation was made for core A1 and core A2 separately, and then the whole matrix was merged. This was done because imputation of the missing values using all variables at once led to variation in the results of the subsequent statistical methods. Table A5 presents the merged matrix produced with the seed 023.

Thereafter, since most variables presented significant correlation to the depth, to evaluate cause effect relationships between MPs and the community of benthic foraminifera, a comparison of the following two models was made:

$$(1)\ Variable = \beta_0 + \beta_1 * Depth$$

$$(2)\ Variable = \beta_0 + \beta_1 * Depth + \beta_2 * MPs$$

An ANOVA test was made to compare these models for all variables, where the null hypothesis was that $\beta_2 = 0$. As shown in Table 5, only triserial test morphology (M5) was best explained by adding MPs to the model (F=7.80, p=0.01). This was also the case for imputation with different seeds.

Table 5. Test statistic and p values for ANOVA test comparing two models for the foraminifera variables with the seed 023. H, P, and A represent hyaline, porcelaneous, and agglutinated tests, respectively. AEI is the *Ammonia-Elphidium* index. M1 to M12 are the morphologies identified for the community of foraminifera. In blue, the values representing rejection of the null hypothesis.

	Forams/g	H	P	A	*Ammonia*	AEI	M1	M2	M3
F	0.67	2.11	1.58	1.30	0.04	2.21	1.42	0.24	2.35
Pr(>F)	0.42	0.16	0.22	0.27	0.84	0.15	0.25	0.63	0.14

Table 5. Continuation

	M4	M5	M6	M7	M8	M9	M10	M11	M12
F	0.82	7.80	0.63	0.75	0.11	0.64	0.35	0.00	0.18
Pr(>F)	0.38	0.01	0.44	0.40	0.74	0.43	0.56	0.97	0.68

In addition, a variable selection was made for the possible multiple linear models that explain the variables with the adjusted R^2 as the criterion. This was achieved using the function *StepCriterion* of the package *glmtoolbox* in the mode *forwardselection*. As shown in Table A6, some inconsistencies arose by the use of different seeds. However, for the most consistent and good models among the example seeds, variability in foraminifera was best explained by changes in granulometry, total carbon, and total nitrogen in the sediment. Once again, M5 was best explained using MPs as one independent variable. For the seed 023, the model for M5 was:

$$M5 = 6.293 + 1.537e^{-04} * MPs - 9.040e^{-02} * TC - 1.750e^{-02} * VFS$$

Where, the adjusted R^2=0.416 (p=0.006637), and only β_1 and β_2 were significant for α=0.05. For some other variables, MPs were included in the model, but with no significance for that variable. Alternatively, MPs were included in the model, with significance, but only for some seeds, which was considered inconsistent. This was the case for TC and TN as well, which consistently depended only on granulometry and between them.

Consequently, statistical analyses point to no significant influence of MPs on the sediment chemistry and the community of benthic foraminifera. Only the relative abundance of triserial tests seems to be influenced by the abundance of this pollutant; however, this result should be taken prudently for the low relative abundance values as discussed in section 2.6. In general, the foraminifera seem to be responding to other changes in the environment, such as those of TC, TN, and granulometry.

3.2 Further considerations

Even though the community of benthic foraminifera seem to have responded over time to changes in oxygenation, OM and water energy, something is causing a trend change in several foraminifera variables (Figure 9) at around 20 cm depth (approximately in 2003), which do not seem to be explained by these variables. In the last decades, several anthropogenic changes have taken place; pollutants have increased their concentration in the marine environment,

and MPs are one of the potential sources of stress for this community and might play a role in this event. Even though the appearance of MPs in the study area seems to be posterior (around 2010, Figure 6), their absence before that time is apparent considering the restrains of the methodology, as detailed in section 1.5.1. Notably, MPs presence down the core in 1978±15 (at around 45 cm) might be related to the peak presented by test wall type, *Ammonia*, AEI, and some morphologies.

Despite the statistical analyses, and the relative low concentration of MPs compared to the high total abundance of benthic foraminifera (maximum value of MP concentration was 5.36 items/g vs the maximum abundance of benthic foraminifera that was 19,785 tests/g), the influence that this pollutant on the community of benthic foraminifera should not be discarded yet. It is encouraged that future studies include analyses such as:

- Identification of foraminifera to species level, which would allow detecting whether diversity decreases while foraminifera abundance increases. This has been recognized as a sign of pollution (Murray, 2006); in addition, the effect of MPs might become visible at this finer taxonomic level (See section 2.5).
- The calculation of indexes such as the EBFOI, TROX, and BFS can contribute to a more comprehensive understanding of the factors that control the community of benthic foraminifera over time (Kranner et al., 2022; Pérez-Asensio & Rodríguez-Ramírez, 2020).
- An assessment of species with triserial tests (M5) should be performed and further studied since their relative abundances was influenced by the concentration of MPs. This, however, should be taken prudently since its relative abundances is lower than 1% and are thus close to confidence limits (Murray, 2006).
- Identification of deformed tests throughout the core might be related with MPs concentration, as it is related to other type of pollutants (Alves Martins et al., 2019; Suokhrie & Saraswat, 2017), and it is worth considering.
- More detailed geochemical analyses might help elucidate the historical influence of MPs in the sediment (section 1.5.1), which is determinant to the composition of the community of benthic foraminifera.

Considering these aspects in the future is recommended to gain deeper understanding on the emerging field of the influence of MPs in the community of benthic foraminifera over time. In addition, other pollutants such as heavy metals might be disturbing the environment and these

organisms, which should be taken into account for further pollution assessments (Suokhrie & Saraswat, 2017).

4. Conclusions and recommendations

4.1 Conclusions

The historical influence of microplastic (MP) presence on the community of benthic foraminifera was evaluated using two sediment cores from Ciénaga de los Vásquez, an open marine lagoon in Cartagena, Colombia. The concentration of MPs increased over time reaching 5358 items/kg in the year 2021±0.31. While this concentration of particles appears higher than previously reported levels in Colombia—where the detection limit has been around 400 µm—the employed methodology, utilizing Nile Red-induced fluorescence of MPs under 365 nm light and automatic counting with ImageJ, allowed the detection of MPs down to 44.27 µm. The reported concentrations correspond to EPS, PP, LDPE, weathered HDPE, and virgin PE as per the detection range of the used methodology, which excluded common polymers such as PET.

Along the core, no significant relationship was found between MPs and total carbon and nitrogen. However, it is recommended to measure inorganic and organic carbon and nitrogen species (e.g., NH_4^+, NO_2^-, NO_3^-, and organic nitrogen) to best understand the historical effects of MPs on the carbon cycle and nitrogen fixation and denitrification processes.

The community of benthic foraminifera exhibited considerable changes over time. Most of them were primarily related to a decrease in grain size coupled with an increase in organic matter in the sediment and changes in its oxygenation. Statistical analyses suggest that MPs do not exert any influence on most of the community of benthic foraminifera; however, a detailed species-level identification is strongly recommended for future studies in this emerging field since the effect of MPs on the community of foraminifera might become more evident at this finer taxonomic level.

Moreover, the observed changes in the community of benthic foraminifera might be linked to other pollutants like heavy metals, which should be analyzed for a more comprehensive understanding.

4.2 Recommendations

Future studies should include analyses such as detailed grain size distribution with laser diffraction, sediment porosity, X-ray fluorescence spectrometry, magnetic susceptibility, or other geochemical analyses to enhance the accuracy of core correlation (Arias-Ortiz et al., 2018; IAEA, 2012; Klootwijk et al., 2021; Turner et al., 2019). In addition, the use of 470 nm light coupled with an orange filter is recommended to improve MPs recovery; under this wavelength a broader range of polymer types present fluorescence when stained with Nile Red dye (Prata et al., 2019b). Moreover, Fourier transform infrared spectroscopy (FTIR) and Raman spectroscopy are advised techniques for obtaining thorough MP profiles since they allow the characterization of polymer types, which could improve historic analysis in combination with core dating techniques (Liu et al., 2022) and could enhance understanding on the effects on sediment chemistry. Other benthic organisms, such as ostracods, could be considered for pollution assessments in the future; their outer shells also remain in the sediment after their death (Camacho & Longobucco, 2007) and are highly abundant in this area. The removal of the outer ring of the sediment during core slicing is advised to avoid the counting of pollutants brought deep in the sediment from the surface (IAEA, 2021). Finally, spatial surficial MP analysis is suggested to understand the differential influence of MP related to sediment facies and its influence on benthic organisms, such as foraminifera.

4.3 Sample and collections availability statement

For future studies in this area, the remaining samples from cores A1 and A2 are available at INVEMAR. Additionally, cores B1 and B2, taken near A1 and A2, are also available for study (Figure 18). Further details on the available material on these cores can be provided upon request.

Please note that surficial total nitrogen, organic carbon, and inorganic carbon measurements were made for samples at 10 different locations within the study area (Figure 18) following the sample locations of Miranda & Parada Ruffinatti (1987). However, these data were not used in the current study as they were obtained during a separate campaign where microplastic measurements were not conducted. If needed, loss on ignition results for cores A1 and B1 can be provided upon request.

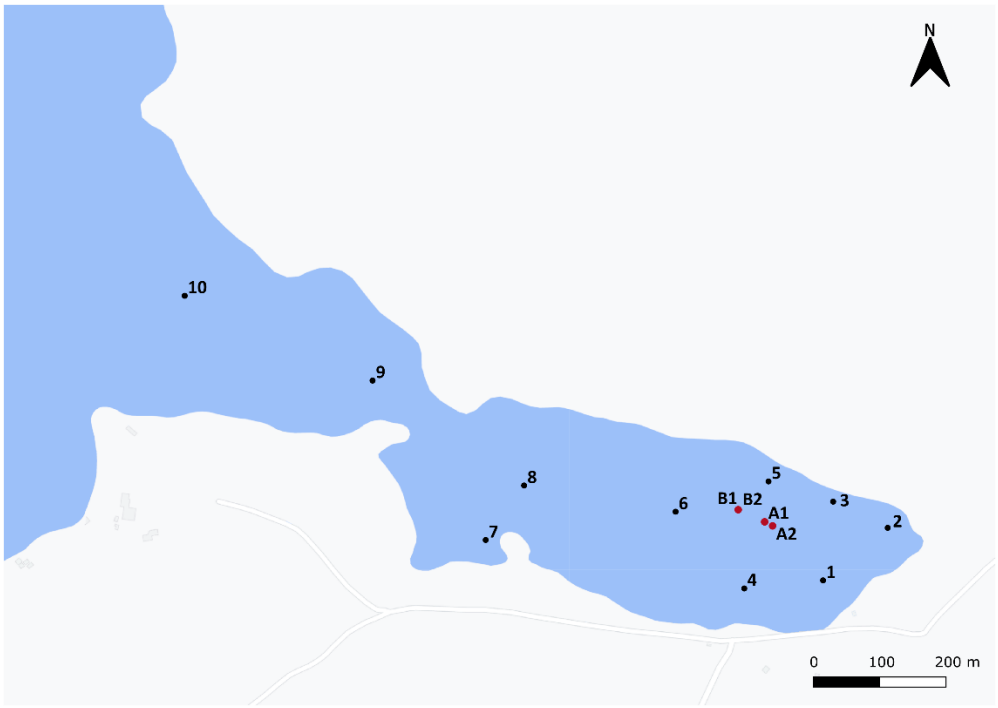

Figure 18. Location of surficial sample points and cores B1 and B2, which are available for future studies.

A collection of the analyzed foraminifera from core A2 is available at MAKURIWA museum at INVEMAR, Santa Marta. Moreover, a collection of foraminifera from the ten surficial samples (Figure 18) is available for reference at the Geology department of Universidad Nacional de Colombia, Bogotá.

Bibliography

Acoplásticos. (n.d.). *Nuestra asociación, quiénes somos*. Retrieved August 16, 2022, from https://www.acoplasticos.org/index.php/mnu-nos/mnu-nos-nta-aso

Acosta-Coley, I., Duran-Izquierdo, M., Rodriguez-Cavallo, E., Mercado-Camargo, J., Mendez-Cuadro, D., & Olivero-Verbel, J. (2019). Quantification of microplastics along the Caribbean Coastline of Colombia: Pollution profile and biological effects on Caenorhabditis elegans. *Marine Pollution Bulletin*, *146*(June), 574–583. https://doi.org/https://doi.org/10.1016/j.marpolbul.2019.06.084

Acosta-Herrera, N. C. (2004). *Compendio Foraminíferos de Colombia*. Universidad Nacional de Colombia.

Acosta, K. (2012). Cartagena, entre el progreso industrial y el rezago social. In *Documentos de Trabajo Sobre Economía Regional*. Banco de la República. https://www.banrep.gov.co/sites/default/files/publicaciones/archivos/dtser_178.pdf

Alves Martins, M. V., Hohenegger, J., Martínez-Colón, M., Frontalini, F., Bergamashi, S., Laut, L., Belart, P., Mahiques, M., Pereira, E., Rodrigues, R., Terroso, D., Miranda, P., Geraldes, M. C., Villena, H. H., Reis, T., Socorro, O. A. A., de Mello e Sousa, S. H., Yamashita, C., & Rocha, F. (2020). Ecological quality status of the NE sector of the Guanabara Bay (Brazil): A case of living benthic foraminiferal resilience. *Marine Pollution Bulletin*, *158*(111449). https://doi.org/10.1016/j.marpolbul.2020.111449

Alves Martins, M. V., Yamashita, C., de Mello e Sousa, S. H., Machado Koutsoukos, E. A., Trevisan Disaró, S., Debenay, J.-P., & Duleba, W. (2019). Response of Benthic Foraminifera to Environmental Variability: Importance of Benthic Foraminifera in Monitoring Studies. In *Monitoring of Marine Pollution* (pp. 225–240). https://doi.org/http://dx.doi.org/10.5772/intechopen.81658

Arias-Ortiz, A., Masqué, P., Garcia-Orellana, J., Serrano, O., Mazarrasa, I., Marbá, N., Lovelock, C. E., Lavery, P. S., & Duarte, C. M. (2018). Reviews and syntheses: 210Pb-derived sediment and carbon accumulation rates in vegetated coastal ecosystems - Setting the record straight. *Biogeosciences*, *15*(22), 6791–6818. https://doi.org/10.5194/bg-15-6791-2018

Birarda, G., Buosi, C., Caridi, F., Casu, M. A., De Giudici, G., Di Bella, L., Medas, D., Meneghini, C., Pierdomenico, M., Sabbatini, A., Surowka, A., & Vaccari, L. (2021). Plastics, (bio)polymers and their apparent biogeochemical cycle: An infrared spectroscopy study on foraminifera. *Environmental Pollution*, *279*, 116912. https://doi.org/10.1016/j.envpol.2021.116912

Bouchet, V. M. P., Seuront, L., Tsujimoto, A., Richirt, J., Frontalini, F., Tsuchiya, M., Matsuba, M., & Nomaki, H. (2023). Foraminifera and plastic pollution: Knowledge gaps and research opportunities. *Environmental Pollution*, *324*(January), 121365. https://doi.org/10.1016/j.envpol.2023.121365

Camacho, H., & Longobucco, M. (2007). *Los invertebrados Fósiles* (1a ed.).

Capolungo, C., Genovese, D., Montalti, M., Rampazzo, E., Zaccheroni, N., & Prodi, L. (2021). Photoluminescence-Based Techniques for the Detection of Micro- and Nanoplastics. *Chemistry—A European Journal*, *27*, 17529–17541. https://doi.org/doi.org/10.1002/chem.202102692 Abstract:

Carnahan, E. A., Hoare, A. M., Hallock, P., Lidz, B. H., & Reich, C. D. (2009). Foraminiferal assemblages in Biscayne Bay, Florida, USA: Responses to urban and agricultural influence in a subtropical estuary. *Marine Pollution Bulletin*, *59*(8–12), 221–233. https://doi.org/10.1016/j.marpolbul.2009.08.008

Carson, H. S., Colbert, S. L., Kaylor, M. J., & McDermid, K. J. (2011). Small plastic debris changes water movement and heat transfer through beach sediments. *Marine Pollution Bulletin*, *62*(8), 1708–1713. https://doi.org/10.1016/j.marpolbul.2011.05.032

Colton Jr, J. B., Burns, B. R., & Knapp, F. D. (1974). Plastic Particles in Surface Waters of the Northwestern Atlantic: The abundance, distribution, source, and significance of various types of plastics are discussed. *Science*, *185*(4150), 491–497. https://science.sciencemag.org/content/185/4150/491

Ding, Y., & Ying, S. (2015). Cell Structure, Density and Impact Strength of Cellulose Acetate Foamed with Supercritical Carbon Dioxide. *Cellular Polymers*, *34*(6), 339–352. https://doi.org/10.1177/026248931503400603

Feldmeijer, W., Metcalfe, B., Scussolini, P., & Arthur, K. (2013). The effect of chemical pretreatment of sediment upon foraminiferal-based proxies. *Geochemistry, Geophysics, Geosystems*, *14*(10), 3996–4014. https://doi.org/10.1002/ggge.20233

Frias, J., & Nash, R. (2019). Microplastics: Finding a consensus on the definition. *Marine Pollution Bulletin*, *138*, 145–147. https://doi.org/10.1016/j.marpolbul.2018.11.022

Frias, J., Pagter, E., Nash, R., O'Connor, I., Carretero, O., Filgueiras, A., Viñas, L., Gago, J., Antunes, J., Bessa, F., Sobral, P., Goruppi, A., Tirelli, V., Pedrotti, M. L., Suaria, G., Aliani, S., Lopes, C., Raimundo, J., Caetano, M., … Gerdts, G. (2018). Standardised protocol for monitoring microplastics in sediments. *JPI-Oceans BASEMAN Project*, *May*, 33. https://doi.org/10.13140/RG.2.2.36256.89601/1

Galindo, A., Costa-Redondo, L. C., Vasco-Echeverri, O., & Arana, V. A. (2023). Microplastic pollution in coastal areas of Colombia: Review. *Marine Environmental Research*, *190*(June). https://doi.org/10.1016/j.marenvres.2023.106027

Galloway, T. S., Cole, M., & Lewis, C. (2017). Interactions of microplastic debris throughout the marine ecosystem. *Nature Ecology and Evolution*, *1*, 1–8. https://doi.org/10.1038/s41559-017-0116

Garcés-Ordóñez, O., Castillo-Olaya, V. A., Granados-Briceño, A. F., Blandón García, L. M., & Espinosa Díaz, L. F. (2019). Marine litter and microplastic pollution on mangrove soils of the Ciénaga Grande de Santa Marta, Colombian Caribbean. *Marine Pollution Bulletin*, *145*(2), 455–462. https://doi.org/10.1016/j.marpolbul.2019.06.058

Garcés-Ordóñez, O., Espinosa, L. F., Costa Muniz, M., Salles Pereira, L. B., & Meigikos dos Anjos, R. (2021). Abundance, distribution, and characteristics of microplastics in coastal surface waters of the Colombian Caribbean and Pacific. *Environmental Science and Pollution Research*, *28*(32), 43431–43442. https://doi.org/10.1007/s11356-021-13723-x

Garcés-Ordóñez, O., Saldarriaga-Vélez, J. F., Espinosa-Díaz, L. F., Canals, M., Sánchez-Vidal, A., & Thiel, M. (2022). A systematic review on microplastic pollution in water, sediments, and organisms from 50 coastal lagoons across the globe. *Environmental Pollution*, *315*(September). https://doi.org/10.1016/j.envpol.2022.120366

Grefstad, A. I. (2019). *Marine benthic foraminifera and microplastics Accumulation and effects following short-and long-term exposure* [Universitetet i Oslo]. http://www.duo.uio.no/

Hallock, P. (2012). The FoRAM Index revisited: uses, challenges, and limitations. *Proceedings of the 12th International Coral Reef …*, *July*, 9–13. http://www.icrs2012.com/proceedings/manuscripts/ICRS2012_15F_2.pdf

Haynes, J. R. (1981). *Foraminifera*.

Hayward, B. W., Holzmann, M., Pawlowski, J., Parker, J. H., Kaushik, T., Toyofuku, M. S., & Tsuchiya, M. (2021). Molecular and morphological taxonomy of living Ammonia and related taxa (Foraminifera) and their biogeography. *Micropaleontology*, *67*(2), 109–313. https://doi.org/10.47894/mpal.67.2-3.01

Hidalgo-Ruz, V., Gutow, L., Thompson, R. C., & Thiel, M. (2012). Microplastics in the marine environment: A review of the methods used for identification and quantification. *Environmental Science and Technology*, *46*(6), 3060–3075. https://doi.org/10.1021/es2031505

Hope, J. A., Coco, G., & Thrush, S. F. (2020). Effects of Polyester Microfibers on Microphytobenthos and Sediment-Dwelling Infauna. *Environmental Science and Technology*, *54*(13), 7970–7982. https://doi.org/10.1021/acs.est.0c00514

IAEA. (2012). *Radiocronología de Sedimentos Costeros Utilizando 210Pb: Modelos, Validación y Aplicaciones*. 118. http://www.researchgate.net/publication/234076951_Radiocronologia_de_Sedimentos_Costeros_Utilizando_210Pb_Modelos_Validacion_y_Aplicaciones/file/32bfe50ededce8cb3e.pdf

IAEA. (2021). *Guía Para el Uso de Sedimentos en la Reconstrucción Histórica de la Contaminación en Zonas Costeras IAEA-TECDOC-1953*. https://doi.org/ISBN 978-92-0-333721-2

INVEMAR. (2003). *Manual de técnicas analíticas para la determinación de parámetros fisicoquímicos y contaminantes marinos (agua, sedimentos y organismos)*. Instituto de Investigaciones Marinas y Costeras. www.invemar.org.co

ISO 10694. (1995). *ISO 10694:1995 - Soil quality — Determination of organic and total carbon after dry combustion (elementary analysis)* (p. 5). International Organization for Standardization. https://www.iso.org/standard/18782.html

ISO 11464. (2006). *Soil quality — Pretreatment of samples for physico-chemical analysis* (p. 11). International Organization for Standardization. https://www.iso.org/standard/37718.html

ISO 13878. (1998). *Soil quality — Determination of total nitrogen content by dry combustion ("elemental analysis")* (p. 7). International Organization for Standardization. https://www.iso.org/standard/23117.html

Jones, R. W. (2014). *Foraminifera and their applications*. Cambridge University Press, New York. https://doi.org/10.1017/CBO9781139567619

Klootwijk, A. T., Alve, E., Hess, S., Renaud, P. E., Sørlie, C., & Dolven, J. K. (2021). Monitoring environmental impacts of fish farms: Comparing reference conditions of sediment geochemistry and benthic foraminifera with the present. *Ecological Indicators*, *120*. https://doi.org/10.1016/j.ecolind.2020.106818

Kranner, M., Harzhauser, M., Beer, C., Auer, G., & Piller, W. E. (2022). Calculating dissolved marine oxygen values based on an enhanced Benthic Foraminifera Oxygen Index. *Scientific Reports*, *12*(1), 1–13. https://doi.org/10.1038/s41598-022-05295-8

Krishnaswamy, S., Lal, D., Martin, J. M., & Meybeck, M. (1971). Geochronology of lake sediments. *Earth and Planetary Science Letters*, *11*(1–5), 407–414. https://doi.org/10.1016/0012-821X(71)90202-0

Kutralam-Muniasamy, G., Pérez-Guevara, F., Elizalde-Martínez, I., & Shruti, V. C. (2020). Review of current trends, advances and analytical challenges for microplastics contamination in Latin America. *Environmental Pollution*, *267*. https://doi.org/10.1016/j.envpol.2020.115463

Ladewig, S. M., Bianchi, T. S., Coco, G., Hope, J. A., & Thrush, S. F. (2021). A call to evaluate Plastic's impacts on marine benthic ecosystem interaction networks. *Environmental Pollution*, *273*, 116423. https://doi.org/10.1016/j.envpol.2021.116423

Lakatos, Á., & Kalmár, F. (2013). Investigation of thickness and density dependence of thermal conductivity of expanded polystyrene insulation materials. *Materials and Structures*, *46*(7), 1101–1105. https://doi.org/10.1617/s11527-012-9956-5

Lavoy, M., & Crossman, J. (2019). A Novel Method for Organic Matter Removal from Samples Containing Microplastics. *Science of the Total Environment*, 135907. https://doi.org/10.1016/j.envpol.2021.117357

Lebreton, L. C. M., van der Zwet, J., Damsteeg, J.-W., Slat, B., Andrady, A., & Reisser, J. (2017). River plastic emissions to the world's oceans. *Nature Communications*, *8*(1), 15611. https://doi.org/10.1038/ncomms15611

Lee, M., & Kim, H. (2022). COVID-19 Pandemic and Microplastic Pollution. *Nanomaterials*, *12*(5). https://doi.org/10.3390/nano12050851

Libes, S. M. (2009). Introduction to marine biochemistry. In Elsevier Science (Ed.), *Jurnal Penelitian Pendidikan Guru Sekolah Dasar* (Second, Vol. 6, Issue August).

Lin, J., Xu, X. M., Yue, B. Y., Xu, X. P., Liu, J. Z., Zhu, Q., & Wang, J. H. (2021). Multidecadal records of microplastic accumulation in the coastal sediments of the East China Sea. *Chemosphere*, *270*, 128658. https://doi.org/10.1016/j.chemosphere.2020.128658

Liu, S., Shang, E., Liu, J., Wang, Y., Bolan, N., Kirkham, M. B., & Li, Y. (2022). What have we known so far for fluorescence staining and quantification of microplastics: A tutorial review. *Frontiers of Environmental Science and Engineering*, *16*(1), 1–14. https://doi.org/10.1007/s11783-021-1442-2

Losada Muñoz, D., & Parada Ruffinatti, C. (1986). Foraminíferos bentónicos y su relación con

la materia orgánica particulada en el sedimento. *Caldasia*, *14*(68), 563–584. https://www.jstor.org/stable/23641449

Martin, C., Baalkhuyur, F., Valluzzi, L., Saderne, V., Cusack, M., Almahasheer, H., Krishnakumar, P. K., Rabaoui, L., Qurban, M. A., Arias-Ortiz, A., Masqué, P., & Duarte, C. M. (2020). Exponential increase of plastic burial in mangrove sediments as a major plastic sink. *Science Advances*, *6*(44). https://doi.org/10.1126/sciadv.aaz5593

Martin, J., Lusher, A. L., & Nixon, F. C. (2022). A review of the use of microplastics in reconstructing dated sedimentary archives. *Science of the Total Environment*, *806*(7491), 150818. https://doi.org/10.1016/j.scitotenv.2021.150818

Matsuguma, Y., Takada, H., Kumata, H., Kanke, H., Sakurai, S., Suzuki, T., Itoh, M., Okazaki, Y., Boonyatumanond, R., Zakaria, M. P., Weerts, S., & Newman, B. (2017). Microplastics in sediment cores from Asia and Africa as indicators of temporal trends in plastic pollution. *Archives of Environmental Contamination and Toxicology*, *73*(2), 230–239. https://doi.org/10.1007/s00244-017-0414-9

Meyers, N., Catarino, A. I., Declercq, A. M., Brenan, A., Devriese, L., Vandegehuchte, M., De Witte, B., Janssen, C., & Everaert, G. (2022). Microplastic detection and identification by Nile red staining: Towards a semi-automated, cost- and time-effective technique. *Science of the Total Environment*, *823*, 153441. https://doi.org/10.1016/j.scitotenv.2022.153441

Miranda, C., & Parada Ruffinatti, C. (1987). Distribución del foramínifero Ammonia beccarii (linné) y su relación con algunos parámetros sedimentológicos en la Ciénaga de los Vásquez (Isla Barú, Colombia). *Boletín de Investigaciones Marinas y Costeras*, *17*, 49–60.

Moore, C. J. (2008). Synthetic polymers in the marine environment: A rapidly increasing, long-term threat. *Environmental Research*, *108*(2), 131–139. https://doi.org/10.1016/j.envres.2008.07.025

Murray, J. (1991). *Ecology and palaeoecology of benthic foraminifera*. Harlow: Longman scientific and technical. http://lib.ugent.be/catalog/rug01:000310130

Murray, J. (2006). *Ecology and Applications of Benthic Foraminifera*. Cambridge University Press, New York. www.cambridge.org/9780521828390

Muthu, S. S. (Ed.). (2021). *Microplastics Pollution* (1st ed.). Springer Singapore. https://doi.org/https://doi.org/10.1007/978-981-16-0297-9

Nares, G. S., Thomson, F. T., Thomson, C. W., & Murray, J. (1884). *Report on the scientific results of the voyage of H.M.S. Challenger during the years 1873-76 under the command of Captain George S. Nares ... and the late Captain Frank Tourle Thomson, R.N: Vol. Zoology v.* Neill and company. https://www.biodiversitylibrary.org/item/18396

Nelms, S. E., Duncan, E. M., Broderick, A. C., Galloway, T. S., Godfrey, M. H., Hamann, M., Lindeque, P. K., & Godley, B. J. (2016). Plastic and marine turtles: a review and call for research. *ICES Journal of Marine Science*, *73*(2), 165–181. https://doi.org/10.1093/icesjms/fsv165

Nichols, G. (2009). *Sedimentology and Stratigraphy* (2nd ed.). Wiley-Blackwell. http://www.wiley.com/go/nicholssedimentology

Ortíz Royero, J. C. (2007). Huracanes y tormentas tropicales en el mar Caribe colombiano desde 1900. *Boletín Científico CIOH*, *25*, 54–60.

https://doi.org/10.26640/22159045.162

Parada Ruffinatti, C. (1992). *Comparación morfológica de topotipos de Ammonia beccarii (linne) con especímenes del Caribe colombiano, Golfo de Méjico y Atlántico oeste*.

Parada Ruffinatti, C., Camacho Rodríguez, C., Caro Caro, C. I., González Contreras, L. S., & Miranda, C. (1996). Lagunas Costeras de Barú, Foraminíferos bentónicos y sedimentos. In *Foraminíferos del Pleistoceno - Holoceno en el Caribe Colombiano* (pp. 115–215).

Patel, R. M. (2016). Polyethylene. *Multilayer Flexible Packaging: Second Edition*, 17–34. https://doi.org/10.1016/B978-0-323-37100-1.00002-8

Pérez-Asensio, J. N., & Rodríguez-Ramírez, A. (2020). Benthic Foraminiferal Salinity index in marginal-marine environments: A case study from the Holocene Guadalquivir estuary, SW Spain. *Palaeogeography, Palaeoclimatology, Palaeoecology*, *560*(September), 110021. https://doi.org/10.1016/j.palaeo.2020.110021

Plafcan, M. M., Schwing, P. T., Romero, I. C., Brooks, G. R., Larson, R. A., O'Malley, B. J., & Stallings, C. D. (2024). Benthic foraminifera in Gulf of Mexico show temporal and spatial dynamics of microplastics. *Marine Pollution Bulletin*, *200*(February), 116090. https://doi.org/10.1016/j.marpolbul.2024.116090

Prata, J. C., Alves, J. R., da Costa, J. P., Duarte, A. C., & Rocha-Santos, T. (2020). Major factors influencing the quantification of Nile Red stained microplastics and improved automatic quantification (MP-VAT 2.0). *Science of the Total Environment*, *719*. https://doi.org/10.1016/j.scitotenv.2020.137498

Prata, J. C., da Costa, J. P., Duarte, A. C., & Rocha-Santos, T. (2019). Methods for sampling and detection of microplastics in water and sediment: A critical review. *TrAC - Trends in Analytical Chemistry*, *110*, 150–159. https://doi.org/10.1016/j.trac.2018.10.029

Prata, J. C., Manana, M. J., Duarte, A. C., & Rocha-santos, T. (2020). What Is the Minimum Volume of Sample to Find Sampling of Aveiro Lagoon and Vouga River, Portugal. *Water*, *12*(1219), 1–10.

Prata, J. C., Reis, V., Matos, J. T. V., da Costa, J. P., Duarte, A. C., & Rocha-Santos, T. (2019). A new approach for routine quantification of microplastics using Nile Red and automated software (MP-VAT). *Science of the Total Environment*, *690*, 1277–1283. https://doi.org/10.1016/j.scitotenv.2019.07.060

Pregnolato, L. A., Viana, R. D. A., Passos, C. C., Misailidis, M. L., & Duleba, W. (2018). Ammonia-Elphidium Index as a proxy for marine pollution assessment, Northeast Brazil. *Journal of Sedimentary Environments*, *3*(3), 176–186. https://doi.org/10.12957/jse.2018.38001

Rangel-Buitrago, N., Arroyo-Olarte, H., Trilleras, J., Arana, V. A., Mantilla-Barbosa, E., Gracia C, A., Mendoza, A. V., Neal, W. J., Williams, A. T., & Micallef, A. (2021). Microplastics pollution on Colombian Central Caribbean beaches. *Marine Pollution Bulletin*, *170*(June), 112685. https://doi.org/10.1016/j.marpolbul.2021.112685

Rangel-Buitrago, N., Mendoza, A. V., Mantilla-Barbosa, E., Arroyo-Olarte, H., Arana, V. A., Trilleras, J., Gracia C, A., Neal, W. J., & Williams, A. T. (2021). Plastic pollution on the Colombian central Caribbean beaches. *Marine Pollution Bulletin*, *162*(September), 111837. https://doi.org/10.1016/j.marpolbul.2020.111837

Rangel-Buitrago, N., & Neal, W. J. (2023). A geological perspective of plastic pollution. *Science of The Total Environment*, *893*(April), 164867.

https://doi.org/10.1016/j.scitotenv.2023.164867

Rangel-Buitrago, N., Ochoa, F. L., Rodríguez, R. D. B., Moreno, J. B., Trilleras, J., Arana, V. A., & Neal, W. J. (2023). Decoding plastic pollution in the geological record: A baseline study on the Caribbean Coast of Colombia, north South America. *Marine Pollution Bulletin*, *192*(April). https://doi.org/10.1016/j.marpolbul.2023.114993

Rocha-Santos, T., Costa, M. F., & Mouneyrac, C. (2022). Handbook of Microplastics in the Environment. In *Handbook of Microplastics in the Environment*. Springer. https://doi.org/10.1007/978-3-030-39041-9

Rogers, K. L., Carreres-Calabuig, J. A., Gorokhova, E., & Posth, N. R. (2020). Micro-by-micro interactions: How microorganisms influence the fate of marine microplastics. *Limnology and Oceanography Letters*, *5*(1), 18–36. https://doi.org/10.1002/lol2.10136

Rönnfeld, W. (2008). *Foraminiferen: Ein Katalog typischer Formen*. Institut für Geowissenschaften der Universitat Tübingen.

Sanchez-Cabeza, J. ., & Ruiz-Fernández, A. C. (2012). 210Pb sediment radiochronology: An integrated formulation and classification of dating models. *Geochimica et Cosmochimica Acta*, *82*, 183–200. https://doi.org/10.1016/j.gca.2010.12.024

Saraswati, P. K. (2021). *Foraminiferal micropaleontology for understanding earth's history*. Elsevier. https://doi.org/https://doi.org/10.1016/C2020-0-01137-0

Seeley, M. E., Song, B., Passie, R., & Hale, R. C. (2020). Microplastics affect sedimentary microbial communities and nitrogen cycling. *Nature Communications*, *11*(1), 1–10. https://doi.org/10.1038/s41467-020-16235-3

Sen Gupta, B. K. (2013). Modern Foraminifera. In *Journal of Chemical Information and Modeling*. Kluwer Academic Publishers.

Suokhrie, T., & Saraswat, R. (2017). *Foraminifera as Bio-Indicators of Pollution: A Review of Research Over the Last Decade Abundant presence of foraminifera in the Arabian Sea oxygen minimum zone View project*. *December*. https://www.researchgate.net/publication/317184862

Toro, P. P. V., Ibarra-gutierrez, K., Bernal, C. A., & Díaz, L. F. E. (2021). Accumulation Rates Using the 210Pb Dating Method in a Sediment Core of the Cispatá Bay, a Marine Protected Area in the Southwestern Colombian Caribbean. *Geology, Earth & Marine Sciences*, *3*(2), 1–5. https://doi.org/10.31038/gems.2021322

Turner, S., Horton, A. A., Rose, N. L., & Hall, C. (2019). A temporal sediment record of microplastics in an urban lake, London, UK. *Journal of Paleolimnology*, *61*(4), 449–462. https://doi.org/10.1007/s10933-019-00071-7

Uddin, S., Fowler, S. W., Uddin, M. F., Behbehani, M., & Naji, A. (2021). A review of microplastic distribution in sediment profiles. *Marine Pollution Bulletin*, *163*(November 2020), 111973. https://doi.org/10.1016/j.marpolbul.2021.111973

UNEP. (2016). Marine Litter Vital Graphics. In *United Nations Environment Programme and GRID-Arendal. Nairobi and Arendal*. https://ec.europa.eu/environment/marine/good-environmental-status/descriptor-10/pdf/Marine_litter_vital_graphics.pdf

Wang, X., Xing, Y., Lv, M., Zhang, T., Ya, H., & Jiang, B. (2022). Recent advances on the effects of microplastics on elements cycling in the environment. *Science of the Total Environment*, *849*(July), 157884. https://doi.org/10.1016/j.scitotenv.2022.157884

Yao, P., Zhou, B., Lu, Y. H., Yin, Y., Zong, Y. Q., Chen, M. Te, & O'Donnell, Z. (2019). A review of microplastics in sediments: Spatial and temporal occurrences, biological effects, and analytic methods. *Quaternary International*, *519*(March), 274–281. https://doi.org/10.1016/j.quaint.2019.03.028

Zaborska, A., Carroll, J. L., Papucci, C., & Pempkowiak, J. (2007). Intercomparison of alpha and gamma spectrometry techniques used in 210Pb geochronology. *Journal of Environmental Radioactivity*, *93*(1), 38–50. https://doi.org/10.1016/j.jenvrad.2006.11.007

Zheng, Y., Li, J., Cao, W., Jiang, F., Zhao, C., Ding, H., Wang, M., Gao, F., & Sun, C. (2020). Vertical distribution of microplastics in bay sediment reflecting effects of sedimentation dynamics and anthropogenic activities. *Marine Pollution Bulletin*, *152*(December 2019), 110885. https://doi.org/10.1016/j.marpolbul.2020.110885

A. Appendix: Detailed Results

Table A1. Results of abiotic variables measured along core A1 and A2. TC corresponds to total carbon, TN is the total nitrogen, MPs represent microplastic concentrations. Regarding granulometry in relative abundances, VFS represents very fine sand (between 63 and 125 μm), FS is the fine sand content (between 125 and 250 μm), MS is the medium sand (between 250 and 500 μm), CS is the coarse sand (between 500 and 1000 μm), VCS is the very coarse sand (between 1000 and 2000 μm), and G are the granules in the sample. *These percentages were normalized for the sediment fraction above 63 μm (i.e., excluding the mud content).

Interval (cm)	Core	Dry weight (g)	TC (g/kg d.w.)	TN (mg/g d.w.)	MPs (items/kg)	Core	Mud (%)	VFS (63) (%*)	FS (125) (%*)	MS (250) (%*)	CS (500) (%*)	VCS (1000) (%*)	G (2000) (%*)
0-1	A1	17.5	56.1	1.77	1746	A2	96.17	57.72	19.6	2.01	1.07	0.94	0
1-2	A1	27.54			5368	A2	97.07	65.12	19.95	1.59	0	0	0
2-3	A1	26.93	57.1	1.59	0	A2	97.21	67.5	19.4	1.9	0	0	0
3-4	A1	30.35	55.7	1.57	1337	A2	97.09	66.67	17.04	1.21	0	0	0
4-5	A1	27.17	56.2	1.6	1961	A2	97.2	67.71	17.14	1.43	0	0	0
5-6	A1	29.76				A2	96.38	61.46	19.22	1.37	0	0	0
6-7	A1	31.06	55.6	1.62	0	A2	96.21	64.88	16.37	1.65	0	0	0
7-8	A1	24.38				A2	96.37	56.17	16.3	2.13	0	0	0
8-9	A1	35.13				A2	97.69	64.2	16.08	1.26	0	0	0
9-10	A1	30.98			3751	A2	96.31	64.69	18.64	1.38	0	0	0
10-11	A1	29.24				A2	96.35	61.41	20.57	2.71	0.7	0	0.62
11-12	A1	30.49	53.5	1.71	1505	A2	96.54	60.89	21.29	3.18	0.77	0	0
12-13	A1	29.3				A2	95.71	59.94	23.46	3.66	0.99	0.15	0
13-14	A1	29.56			314	A2	95.64	64.65	20.25	2.99	1.02	0.7	0
14-15	A1	28.6	53.9	1.7	0	A2	95.36	64.02	22.66	2.72	0.42	0.21	0
15-16	A1	30.58				A2	96.55	60.04	22.3	2.94	0.54	0	0
16-17	A1	31.08	53.7	1.66	0	A2	96.15	62.58	22.77	4.06	1.24	0.35	0
17-18	A1	34.46				A2	95.17	59.79	25.42	4.68	1.69	1.17	0
18-19	A1	35.62				A2	94.68	55.35	27.24	6.45	2.31	1.13	0
19-20	A1	32.03	54.4	1.62	0	A2	93.41	49.82	26.96	6.81	0.43	0.87	0.67
20-21	A1	30.88				A2							
21-22	A1	33.36				A2	95.35	59.49	24.51	6.2	2.25	0.79	0.62
22-23	A1	33.14				A2							
23-24	A1	34.41				A2							
24-25	A1	33.7	56.3	1.63	0	A2	95.19	62.11	23.74	4.56	1.45	0.96	0
25-26	A1	52.56				A2							
26-27	A1	39.01				A2	92.5	55.13	28.67	6.67	2.2	1.05	0.28
27-28	A1	34.86				A2							
28-29	A1	36.96				A2							
29-30	A1	38.36			0	A2	91.92	51.82	30.42	7.96	2.44	1.16	0.46
30-31	A1	37.09				A2							
31-32	A1	36.79				A2							
32-33	A1	36.61				A2							

Interval (cm)	Core	Dry weight (g)	TC (g/kg d.w.)	TN (mg/g d.w.)	MPs (items/kg)	Core	Mud (%)	VFS (63) (%*)	FS (125) (%*)	MS (250) (%*)	CS (500) (%*)	VCS (1000) (%*)	G (2000) (%*)
33-34	A1	40.56				A2							
34-35	A1	39.61	55.9	1.44	0	A2	93.1	51.92	29.44	8.93	3.2	1.7	0.43
35-36	A1	41.99				A2							
36-37	A1	36.23				A2							
37-38	A1	40.67				A2							
38-39	A1	40.06				A2							
39-40	A1	36.69	58.6	1.49	311	A2	91.18	48.49	31.17	10.04	3.37	1.34	0.88
40-41	A1	40.85				A2							
41-42	A1	35.87				A2							
42-43	A1	38.56				A2							
43-44	A1	42.49				A2							
44-45	A1	39.74	56.3	1.49	915	A2	92.25	45.59	29.25	9.81	3.7	2.13	0.78
45-46	A1	41.47				A2							
46-47	A1	41.26				A2							
47-48	A1	38.22				A2							
48-49	A1	42.15				A2							
49-50	A1	44.63				A2							
50-51	A1	39.6	58.9	1.37	559	A2	89.99	41.28	33.03	11.79	4.72	2.47	1.17
51-52	A1	41.73				A2							
52-53	A1	44.34				A2							
53-54	A1	40.6				A2							
54-55	A1	41.89				A2							
55-56	A1	44.01				A2							
56-57	A1	46.52				A2							
57-58	A1	41.6				A2							
58-59	A1	46.59				A2							
59-60	A1	58.69				A2							
60-61	A1	55.35	62.9	1.36	0	A2	83.43	37.6	30.5	10.66	4.8	3.72	7.4
61-62	A1	57.71				A2							
62-63	A1	74.31				A2							
63-64	A1	48.82				A2							
64-65	A1	47.46				A2							
65-66	A1	47.78				A2							
66-67	A1	47.66				A2							
67-68	A1	47.48				A2							
68-69	A1	43.25				A2							
69-70	A1	43.32				A2							
70-71	A1	42.19	62.8	1.33	0	A2	85.3	27.93	23.95	9.95	4.27	3.37	24.26
71-72	A1	47.65				A2							
72-73	A1	44.55				A2							
73-74	A1	48.41				A2							
74-75	A1	48.63				A2							
75-76	A1	45.71				A2							
76-77	A1	48.88				A2							
77-78	A1	43.5				A2							
78-79	A1	44.52				A2							
79-80	A1	41.37				A2							
80-81	A1	41.13				A2							
81-82	A1	38.81				A2							
82-83	A1	41.5				A2							
83-84	A1	45.6				A2							
84-85	A1	45.46				A2							
85-86	A1	45.8				A2							
86-87	A1	46.78				A2							
87-88	A1	48.25				A2							
88-89	A1	42.85				-							

Interval (cm)	Core	Dry weight (g)	TC (g/kg d.w.)	TN (mg/g d.w.)	MPs (items/kg)	Core	Mud (%)	VFS (63) (%*)	FS (125) (%*)	MS (250) (%*)	CS (500) (%*)	VCS (1000) (%*)	G (2000) (%*)
89-90	A1	46.69				-							
90-91	A1	43.85				-							
91-92	A1	42.79				-							
92-93	A1	41.79				-							
93-94	A1	37.35				-							

Table A2. Radiometric data and ages of core A1 using the constant flux-constant sedimentation model (CF:CS). Where $\mathbf{m_i}$ represents massic depth as shown in Figure 5, $\mathbf{^{210}Pb_{tot}}$ is the total ^{210}Pb activity, $\mathbf{u(^{210}Pb_{tot})}$ is the uncertainty of total ^{210}Pb activity, $\mathbf{^{210}Pb_{supp}}$ is the supported ^{210}Pb, which was obtained by averaging $^{210}Pb_{tot}$ in the eight deepest analyzed samples, $\mathbf{u(^{210}Pb_{supp})}$ is the uncertainty of supported ^{210}Pb corresponding to the standard deviation of the eight deepest analyzed samples, $\mathbf{^{210}Pb_{ex}}$ is the excess ^{210}Pb (also known as unsupported ^{210}Pb) calculated by subtracting supported ^{210}Pb from $^{210}Pb_{tot}$, $\mathbf{u(^{210}Pb_{ex})}$ is the uncertainty of $^{210}Pb_{ex}$, **Age (yr)** represents the calculated ages for intervals with unsupported ^{210}Pb according to the CF:CS model, and **u(Age)** is the uncertainty of calculated ages.

Interval (cm)	m_i (g cm^{-2})	$^{210}Pb_{tot}$ (Bq kg^{-1})	u($^{210}Pb_{tot}$) (Bq kg^{-1})	$^{210}Pb_{supp}$ (Bq kg-1)	u($^{210}Pb_{supp}$) (Bq kg-1)	$^{210}Pb_{ex}$ (Bq kg^{-1})	u($^{210}Pb_{ex}$) (Bq kg^{-1})	Age (yr)	u (Age)
1-2	0.54	20.98	1.7	11.5	0.4	9.5	1.8	2021	0.3
5-6	2.51	15.50	1.7	11.5	0.4	4.0	1.8	2018	1.4
12-13	6.17	23.61	1.9	11.5	0.4	12.1	1.9	2012	3.5
24-25	12.87	21.93	1.8	11.5	0.4	10.4	1.8	2001	7.3
31-32	17.63	21.35	1.7	11.5	0.4	9.8	1.8	1993	10.0
44-45	26.46	18.53	1.5	11.5	0.4	7.0	1.5	1978	15.0
47-48	28.58	12.55	1.5	11.5	0.4	1.0	1.5	1974	16.2
50-51	30.76	14.10	1.1	11.5	0.4	2.6	1.1	1971	17.4
54-55	33.67	12.53	1.0	11.5	0.4	1.0	1.0	1966	19.1
58-59	36.74	13.40	1.0	11.5	0.4	1.9	1.1	1961	20.8
59-60	37.65	11.61	0.9	11.5	0.4				
61-62	39.62	10.69	0.8	11.5	0.4				
70-71	47.44	11.73	0.9	11.5	0.4				
74-75	50.68	13.73	1.0	11.5	0.4				
77-78	53.11	11.71	0.9	11.5	0.4				
84-85	58.28	11.29	1.2	11.5	0.4				
88-89	61.50	11.17	0.9	11.5	0.4				
92-93	64.55	11.92	0.9	11.5	0.4				

Table A3. Summary of microplastic contents in core A1. The results were obtained using the code MP-VAT 2.0A as explained in Section 1.3.2. Samples with a "D" represent the duplicates of each badge. In Blank subtraction, underlined values represent the first badge with corresponding Blank 1. Reported value corresponds to the blank subtraction, wherein negative values were adjusted to zero. The detection limit was calculated from image resolution and the lower limit of the code (three pixels). The code provides an approximation of the smallest and largest dimension of each plastic particle, which correspond to MinFeret and MaxFeret, respectively, as detailed in (Prata et al., 2019b). The average and standard deviation of MaxFeret are provided as well.

Sample	Sediment dry weight (g)	MP-VAT 2.0A Counted particles	Blank subtraction	Reported value	Detection limit (µm)	Reported items/kg d.w.	Min Feret (µm)	Max Feret (µm)	Avg MaxFeret (µm)	SD MaxFeret (µm)
0-1	8.017	20	14	14	44.64	1746	63	512	141.4	112.9
1-2	8.197	50	44	44	43.48	5368	52	1013	168.4	144.3
2-3	8.224	3	-3	0	44.85	0	-	-	-	-
3-4	8.225	17	11	11	43.95	1337	98	302	201.6	63.5
4-5	8.160	22	16	16	43.98	1961	66	270	141.0	55.9
6-7	9.367	2	-3	0	43.73	0	-	-	-	-
9-10	8.265	37	31	31	44.09	3751	53	501	182.5	90.2
11-12	9.301	19	14	14	43.73	1505	46	403	148.2	105.5
13-14	9.560	8	3	3	44.06	314	126	265	196.0	69.5
14-15	8.063	6	-1.5	0	44.23	0.0	-	-	-	-
14-15D	8.011	3		0	44.06		-	-	-	-
16-17	10.105	5	0	0	43.88	0.0	-	-	-	-
19-20	8.264	4	-2	0	44.26	0.0	-	-	-	-
24-25	8.271	3	-3	0	43.95	0.0	-	-	-	-
29-30	8.086	4	-2	0	43.95	0.0	-	-	-	-
34-35	9.410	4	-1.5	0	47.32	0.0	-	-	-	-
34-35D	9.437	3		0	44.40		-	-	-	-
39-40	9.660	8	3	3	44.51	310.6	46	247	145.7	100.5
44-45	8.741	13	8	8	43.73	915.2	66	333	158.5	90.9
50-51	8.950	10	5	5	44.40	558.7	99	829	317.2	292.6
60-61	9.156	4	-1	0	43.99	0.0	-	-	-	-
70-71	9.363	4	-1	0	44.40	0.0	-	-	-	-
Blank 1	0.000	6								
Blank 2	0.000	5								

Table A4. Results of biotic variables measured along core A2. H represents the relative abundance of hyaline tests, P is that of porcelaneous tests, and A is the relative abundance of agglutinated tests. *Ammonia* represents the relative abundance of the genus *Ammonia*; AEI is the *Ammonia-Elphidium* index. M1 corresponds to the relative abundance of tests with miliolid coiling; M2, trochospiral coiling; M3, planispiral involute coiling; M4, biserial tests; M5: triserial tests; M6, uniserial tests; M7, planispiral evolute coiling; M8: spiral to serial tests; M9, single chambered tests; M10, cyclic annular-discoidal tests; M11, tri- bi- to uniserial tests; and M12, tests of the superfamily Soritoidea.

Interval (cm)	Forams/g	H (%)	P (%)	A (%)	*Ammonia (%)*	AEI	M1 (%)	M2 (%)	M3 (%)	M4 (%)	M5 (%)	M6 (%)	M7 (%)	M8 (%)	M9 (%)	M10 (%)	M11 (%)	M12 (%)
0-1	12545.5	52.54	44.57	2.90	28.26	63.41	43.48	34.06	17.75	1.81	0.73	0.36	0.00	0.00	0.73	0.00	0.00	1.087
1-2	16444.4	47.30	51.35	1.35	26.35	66.10	50.34	31.42	14.19	1.35	1.01	0.00	0.34	0.00	0.00	0.34	0.00	1.014
2-3	15500.0	50.97	45.81	3.23	29.03	69.23	44.52	35.48	14.52	3.23	0.00	0.32	0.00	0.00	0.00	0.65	0.00	1.29
3-4	19400.0	49.83	46.74	3.44	28.87	63.64	46.74	33.33	16.50	3.44	0.00	0.00	0.00	0.00	0.00	0.00	0.00	0
4-5	16000.0	47.79	50.37	1.84	28.68	69.64	48.53	34.19	12.87	1.47	0.37	0.00	0.00	0.00	0.00	0.37	0.37	1.838
5-6																		
6-7	16823.5	48.25	50.00	1.75	26.92	65.25	49.30	31.47	15.39	2.10	0.35	0.00	0.70	0.00	0.00	0.00	0.00	0.699
7-8																		
8-9	19785.7	48.01	50.18	1.81	29.96	72.81	49.10	33.21	13.00	2.17	0.36	0.00	0.36	0.00	0.00	0.72	0.00	1.083
9-10	15579.0	53.72	43.92	2.36	29.39	66.92	43.58	35.81	15.88	2.37	1.35	0.00	0.00	0.34	0.34	0.00	0.00	0.338
10-11																		
11-12	9838.7	46.23	51.48	2.30	29.18	72.36	50.16	32.79	12.79	2.30	0.00	0.00	0.33	0.00	0.00	0.00	0.33	1.311
12-13																		
13-14	19333.3	34.77	63.22	2.01	20.12	67.31	62.36	23.28	10.63	2.59	0.00	0.00	0.00	0.00	0.00	0.29	0.00	0.862
14-15	16611.1	41.47	56.19	2.34	28.76	76.79	54.85	31.44	9.37	2.68	0.33	0.00	0.00	0.00	0.00	0.00	0.00	1.338
15-16																		
16-17	12571.4	42.42	54.92	2.65	26.52	72.17	53.79	30.30	11.36	1.14	0.76	0.38	0.38	0.00	0.00	0.38	0.38	1.136
17-18																		
18-19																		
19-20	10629.6	39.02	58.89	2.09	28.57	86.32	57.14	33.45	4.88	1.05	0.70	0.00	0.35	0.00	0.35	0.70	0.00	1.394
20-21																		
21-22																		
22-23																		
23-24																		
24-25	14000.0	34.69	63.61	1.70	21.43	72.41	62.25	24.15	9.86	1.02	0.00	0.34	0.00	0.68	0.00	0.34	0.00	1.361
25-26																		
26-27																		
27-28																		
28-29																		

Interval (cm)	Forams/g	H (%)	P (%)	A (%)	*Ammonia (%)*	AEI	M1 (%)	M2 (%)	M3 (%)	M4 (%)	M5 (%)	M6 (%)	M7 (%)	M8 (%)	M9 (%)	M10 (%)	M11 (%)	M12 (%)
29-30	9906.3	37.22	60.25	2.52	20.50	63.11	58.36	22.40	12.93	2.52	0.63	0.00	0.63	0.00	0.00	0.63	0.00	1.893
30-31																		
31-32																		
32-33																		
33-34																		
34-35	7891.9	41.10	55.82	3.08	18.84	57.90	53.77	24.66	16.10	3.08	0.00	0.00	0.34	0.00	0.00	0.00	0.00	2.055
35-36																		
36-37																		
37-38																		
38-39																		
39-40	8675.7	30.53	67.60	1.87	16.82	62.07	65.73	19.63	10.28	1.56	0.00	0.31	0.00	0.00	0.00	0.62	0.00	1.869
40-41																		
41-42																		
42-43																		
43-44																		
44-45	5660.4	49.67	48.67	1.67	25.00	65.79	46.00	34.00	14.67	1.67	0.33	0.00	0.00	0.00	0.00	0.67	0.00	2.667
45-46																		
46-47																		
47-48																		
48-49																		
49-50																		
50-51	6229.2	33.11	64.55	2.34	16.72	58.14	62.88	20.40	12.38	1.67	0.67	0.33	0.00	0.00	0.00	0.00	0.00	1.672
51-52																		
52-53																		
53-54																		
54-55																		
55-56																		
56-57																		
57-58																		
58-59																		
59-60																		
60-61	3413.0	32.80	63.69	3.50	12.10	46.34	62.42	16.24	16.24	3.19	0.00	0.32	0.00	0.00	0.00	0.32	0.00	1.274
61-62																		
62-63																		
63-64																		

Interval (cm)	Forams/g	H (%)	P (%)	A (%)	*Ammonia (%)*	AEI	M1 (%)	M2 (%)	M3 (%)	M4 (%)	M5 (%)	M6 (%)	M7 (%)	M8 (%)	M9 (%)	M10 (%)	M11 (%)	M12 (%)
64-65																		
65-66																		
66-67																		
67-68																		
68-69																		
69-70																		
70-71	4618.4	32.48	66.67	0.86	8.55	34.09	64.67	13.39	17.66	0.86	0.00	0.00	0.00	0.00	0.29	1.14	0.00	1.994
71-72																		
72-73																		
73-74																		
74-75																		
75-76																		
76-77																		
77-78																		
78-79																		
79-80																		
80-81																		
81-82																		
82-83																		
83-84																		
84-85																		
85-86																		
86-87																		
87-88																		

Table A5. Reduced data matrix for statistical analyses. Imputed values are shown in blue. Refer to Table A4 for clarification of the headings.

Interval (cm)	Core	TC (g/kg d.w.)	TN (mg/g d.w.)	MPs (items/kg)	Core	Mud (%)	Forams/g	H (%)	P (%)	A (%)	*Ammonia* (%)	AEI
0-1	A1	56.1	1.77	1746	A2	96.17	12545.5	52.54	44.57	2.90	28.26	63.41
1-2	A1	53.5	1.77	5368	A2	97.07	16444.4	47.30	51.35	1.35	26.35	66.10
2-3	A1	57.1	1.59	0	A2	97.21	15500.0	50.97	45.81	3.23	29.03	69.23
3-4	A1	55.7	1.57	1337	A2	97.09	19400.0	49.83	46.74	3.44	28.87	63.64
4-5	A1	56.2	1.6	1961	A2	97.2	16000.0	47.79	50.37	1.84	28.68	69.64
6-7	A1	55.6	1.62	0	A2	96.21	16823.5	48.25	50.00	1.75	26.92	65.25
8-9	A1	53.9	1.57	0	A2	97.69	19785.7	48.01	50.18	1.81	29.96	72.81
9-10	A1	53.5	1.77	3751	A2	96.31	15579.0	53.72	43.92	2.36	29.39	66.92
11-12	A1	53.5	1.71	1505	A2	96.54	9838.7	46.23	51.48	2.30	29.18	72.36
13-14	A1	53.7	1.7	314	A2	95.64	19333.3	34.77	63.22	2.01	20.12	67.31
14-15	A1	53.9	1.7	0	A2	95.36	16611.1	41.47	56.19	2.34	28.76	76.79
16-17	A1	53.7	1.66	0	A2	96.15	12571.4	42.42	54.92	2.65	26.52	72.17
19-20	A1	54.4	1.62	0	A2	93.41	10629.6	39.02	58.89	2.09	28.57	86.32
24-25	A1	56.3	1.63	0	A2	95.19	14000.0	34.69	63.61	1.70	21.43	72.41
29-30	A1	55.7	1.49	0	A2	91.92	9906.3	37.22	60.25	2.52	20.50	63.11
34-35	A1	55.9	1.44	0	A2	93.1	7891.9	41.10	55.82	3.08	18.84	57.90
39-40	A2	58.6	1.49	311	A2	91.18	8675.7	30.53	67.60	1.87	16.82	62.07
44-45	A1	56.3	1.49	915	A2	92.25	5660.4	49.67	48.67	1.67	25.00	65.79
50-51	A1	58.9	1.37	559	A2	89.99	6229.2	33.11	64.55	2.34	16.72	58.14
60-61	A1	62.9	1.36	0	A2	83.43	3413.0	32.80	63.69	3.50	12.10	46.34
70-71	A1	62.8	1.33	0	A2	85.3	4618.4	32.48	66.67	0.86	8.55	34.09

Interval (cm)	Core	M1 (%)	M2 (%)	M3 (%)	M4 (%)	M5 (%)	M6 (%)	M7 (%)	M8 (%)	M9 (%)	M10 (%)	M11 (%)	M12 (%)
0-1	A2	43.48	34.06	17.75	1.81	0.73	0.36	0.00	0.00	0.73	0.00	0.00	1.09
1-2	A2	50.34	31.42	14.19	1.35	1.01	0.00	0.34	0.00	0.00	0.34	0.00	1.01
2-3	A2	44.52	35.48	14.52	3.23	0.00	0.32	0.00	0.00	0.00	0.65	0.00	1.29
3-4	A2	46.74	33.33	16.50	3.44	0.00	0.00	0.00	0.00	0.00	0.00	0.00	0.00
4-5	A2	48.53	34.19	12.87	1.47	0.37	0.00	0.00	0.00	0.00	0.37	0.37	1.84
6-7	A2	49.30	31.47	15.39	2.10	0.35	0.00	0.70	0.00	0.00	0.00	0.00	0.70
8-9	A2	49.10	33.21	13.00	2.17	0.36	0.00	0.36	0.00	0.00	0.72	0.00	1.08
9-10	A2	43.58	35.81	15.88	2.37	1.35	0.00	0.00	0.34	0.34	0.00	0.00	0.34
11-12	A2	50.16	32.79	12.79	2.30	0.00	0.00	0.33	0.00	0.00	0.00	0.33	1.31
13-14	A2	62.36	23.28	10.63	2.59	0.00	0.00	0.00	0.00	0.00	0.29	0.00	0.86
14-15	A2	54.85	31.44	9.37	2.68	0.33	0.00	0.00	0.00	0.00	0.00	0.00	1.34
16-17	A2	53.79	30.30	11.36	1.14	0.76	0.38	0.38	0.00	0.00	0.38	0.38	1.14
19-20	A2	57.14	33.45	4.88	1.05	0.70	0.00	0.35	0.00	0.35	0.70	0.00	1.39
24-25	A2	62.25	24.15	9.86	1.02	0.00	0.34	0.00	0.68	0.00	0.34	0.00	1.36
29-30	A2	58.36	22.40	12.93	2.52	0.63	0.00	0.63	0.00	0.00	0.63	0.00	1.89
34-35	A2	53.77	24.66	16.10	3.08	0.00	0.00	0.34	0.00	0.00	0.00	0.00	2.06
39-40	A2	65.73	19.63	10.28	1.56	0.00	0.31	0.00	0.00	0.00	0.62	0.00	1.87
44-45	A2	46.00	34.00	14.67	1.67	0.33	0.00	0.00	0.00	0.00	0.67	0.00	2.67
50-51	A2	62.88	20.40	12.38	1.67	0.67	0.33	0.00	0.00	0.00	0.00	0.00	1.67
60-61	A2	62.42	16.24	16.24	3.19	0.00	0.32	0.00	0.00	0.00	0.32	0.00	1.27
70-71	A2	64.67	13.39	17.66	0.86	0.00	0.00	0.00	0.00	0.29	1.14	0.00	1.99

Table A6. Comparison of multivariate linear model for two example matrices (generated by imputation of missing values with different seeds). In gray, *p*-values for the variable MPs where its addition to the model was no significant (α=0.05). In green, the only variable that showed both consistency among the models for different matrices and was significantly influenced by MPs concentration. Refer to table A1 for clarification of the variables' abbreviations.

Variable	Best group of variables (seed 023)	Adjusted R^2	*p*-value	*p*-value for MPS	Shapiro test *p*-value	Best group of variables (seed 999)	Adjusted R^2	*p*-value	*p*-value for MPS	Shapiro test *p*-value
Forams abundance	MS + VFS + N	0.8421	1.24e-07	-	0.8341	MS + VFS + N + MPs	0.8556	2.563e-07	0.165500	0.4424
H	Depth + MPs + FS + MS	0.5455	0.001860	0.143251	0.6813	Depth + MPs + FS + MS	0.5455	0.001860	0.143251	0.6813
P	Depth + MPs + N	0.5199	0.001344	0.120720	0.3303	Depth + MPs	0.5095	0.000637	0.224900	0.8717
A	G + C	0.2066	0.048260	-	0.3055	Mud + Depth + MPs + CS + N + C + VFS	0.3792	0.055110	0.135560	0.8717
Ammonia	Depth + C	0.8006	1.931e-07	-	0.4703	Depth + C	0.8310	4.347e-08	-	0.9095
AEI	G + MPs +CS + MS + N + Depth + Mud + VFS	0.9167	1.151e-06	0.014970	0.1273	G + CS + MS + N + Depth + Mud + VCS	0.9355	5.941e-08	-	0.1244
M1	Depth + MPs + N	0.4774	0.002691	0.134210	0.4095	Depth + MPs	0.4662	0.001363	0.248640	0.7551
M2	Mud + CS + VFS + G + FS	0.7564	4.339e-05	-	0.8576	Mud + CS + VFS + G + FS	0.7564	4.339e-05	-	0.8576
M3	CS + Depth + MPs + N + G + MS	0.6406	0.001399	0.050002	0.6616	FS + CS + Depth + MPs	0.5761	0.001099	0.134090	0.7272
M4	G + N + MS + Mud + FS	0.2951	0.063860	-	0.8886	N + MS + Mud + MPs + FS + CS + Depth + C	0.4560	0.038330	0.035820	0.9287
M5	MPs + C + VFS	0.4161	0.006637	0.007920	0.8168	MPs + C + Mud	0.4161	0.006634	0.001480	0.7790
M6	C + N + MPs + CS + Mud + FS	0.5368	0.006978	0.066733	0.0521	CS + C + MPs + N + G + Mud	0.4694	0.016050	0.086060	0.2378
M7	C + N	0.1836	0.062420	-	0.0596	C + Mud + VCS	0.2945	0.030200	-	0.1943
M8	-	-	-	-	-	-	-	-	-	-
M9	N + VFS + Depth + C + Mud + VCS	0.6638	0.000909	-	0.1149	-	-	-	-	-
M10	G	0.2588	0.010800	-	0.0042	G	0.2588	0.01080	-	0.0042
M11	VCS	0.0428	0.184900	-	1.513e-05	N	0.0491	0.17010	-	3.518e-05

Variable	Best group of variables (seed 023)	Adjusted R^2	*p*-value	*p*-value for MPS	Shapiro test *p*-value	Best group of variables (seed 999)	Adjusted R^2	*p*-value	*p*-value for MPS	Shapiro test *p*-value
M12	MS + Mud + G	0.5375	0.000988	-	0.8181	MS + Mud + G + N	0.5483	0.00178	-	0.4424
C	Mud + FS + N	0.8247	2.991e-07	-	0.0901	Mud + FS + N + MPs	0.8089	2.318e-06	0.163709	0.2055
N	C + MPs + MS + FS + VFS	0.8485	1.37e-06	0.193790	0.4565	MS + FS + VFS + MPs + Mud	0.8493	1.317e-06	0.009360	0.1702

B. Appendix: Microplastic count macro scripts

MP-SCALE

```
//MP-SCALE v1.0A
//Created by J.C.Prata, V. Reis, J. Matos, J.P.da Costa, A.Duarte, T.Rocha-Santos 2019
//Modified by Estefany Andrea Mora Galindo (thus 1.0A instead of 1.0), modifications are shown with **

macro "MPSCALE Action Tool - C000D81D91Da1Cd61D52D62D72C000D82Cd61D92Da2Db2D43Cfc9D53D63D73C000D83Cfc9D93Da3Db3Cd61Dc3D34Cfc9D44D54D64D74C000D84D94Da4Cfc9Db4Dc4Cd61Dd4D25Cfc9D35D45D55D65D75C000D85Cfc9D95Da5Db5Dc5Dd5Cd61De5D26Cfc9D36D46D56D66D76C000D86Cfc9D96Da6Db6Dc6Dd6Cd61De6D27Cfc9D37D47D57D67D77C000D87D97Da7Cfc9Db7Dc7Dd7Cd61De7D28Cfc9D38D48D58D68D78C000D88Cfc9D98Da8Db8Dc8Dd8Cd61De8D29Cfc9D39D49D59D69D79C000D89Cfc9D99Da9Db9Dc9Dd9Cd61De9D2aCfc9D3aD4aD5aD6aD7aC000D8aD9aDaaCfc9DbaDcaDdaCd61DeaD2bCfc9D3bD4bD5bD6bD7bC000D8bCfc9D9bDabDbbDcbDdbCd61DebD3cCfc9D4cD5cD6cD7cC000D8cCfc9D9cDacDbcDccCd61DdcD4dCfc9D5dD6dD7dC000D8dD9dDadCfc9DbdCd61DcdD5eD6eD7eC000D8eCd61D9eDaeDbeC000D8f" {

waitForUser("Set the scale using selection","Use make oval tool to draw a circle over your filter, then click 'OK'");

//Get diameter from circular selection
run("Set Measurements...", "feret's display redirect=None decimal=3");
run("Measure");
result = getResult("Feret");
if (isOpen("Results")) {      selectWindow("Results");      run("Close");
}

//Get information from user
Dialog.create("Know measures");
Dialog.addNumber("Diameter:", 47);
```

```
Dialog.addString("Length unit:", "mm");
diameter = Dialog.getNumber();
lunit = Dialog.getString();
Dialog.show();

//Set scale automatically
run("Set    Scale...",    "distance=result    known=diameter    pixel=1
unit="+lunit+"");

//**Put scale and grid in image file
run("Scale Bar...", "width=5 height=7 thickness=20 font=80 color=White
background=None location=[Lower Right] horizontal bold overlay");
run("Grid...", "grid=Lines area=100 color=Cyan center");

//**Save file as jpg
dir = File.directory;
name = File.nameWithoutExtension;
saveAs("Jpeg", dir + name + ".jpeg");
}
```

MP-VAT 2.0A

MP-VAT 2.0 was created for use with 470 nm light and an orange filter, which blocks or attenuates blue and violet light enhancing the visibility of the red fluorescence emitted by the NR-painted particles. The original script further subtracts the green channel from the red one to count MPs and uses the RenyiEntropy threshold to select MPs particles larger than three pixels. When using 365 nm light (with no orange filter), best results were obtained subtracting the blue channel from the red one in ImageJ when using WB in tungsten mode. Other changes include saving the mask image in the file folder with a scale and grid for reference.

```
//MP-VAT (Microplastics Visual Analysis Tool) version 2.0A
//Created by J.C.Prata, J. R. Alves, V. Reis, J. Matos, J.P.da Costa,
A.Duarte, T.Rocha-Santos 2019
//Modified by Estefany Andrea Mora Galindo (thus 2.0A instead of 2.0),
modifications are shown with ** These include saving the mask image; and
subtracting the blue channel, instead of the green one, to the red one.

macro            "MPVAT2A            Action            Tool            -
C369D32D72D92Da2Db2Dc2D33D43D63D73D93Dd3D34D54D74D94Dd4D35D55D75D95Da5Db
5Dc5D36D76D96D37D77D97D3aD5aD7aD8aD9aDbaDcaDdaD3bD5bD7bD9bDcbD3cD5cD7cD8
cD9cDccD3dD5dD7dD9dDcdD4eD7eD9eDce"{

//Function Red
```

```
//** Blue substraction
function red() {
imageName=getTitle();
setBatchMode(true);
run("Split Channels");
imageCalculator("Subtract create", imageName + " (red)", imageName + "
(blue)");

selectWindow(imageName + " (red)");
close();
selectWindow(imageName + " (blue)");
close();
selectWindow(imageName + " (green)");
close();

selectWindow("Result of " + imageName + " (red)");
}

//Function MP-VAT v1.0
function mpvat() {

//Color inversion, 8-bit conversion and automatic threshold
run("Invert");
run("8-bit");
setAutoThreshold("RenyiEntropy");
setOption("BlackBackground", false);
run("Convert to Mask");

//**Saving mask image with scale and grid
run("Scale Bar...", "width=5 height=7 thickness=8 font=25 color=Blue
background=None location=[Lower Right] horizontal bold overlay");
run("Grid...", "grid=Lines area=100 color=Cyan center");
dir = File.directory;
name = File.nameWithoutExtension;
saveAs("Jpeg", dir + name + "_maskBlue.jpeg");

run("Set Measurements...", "area shape feret's display redirect=None
decimal=3");

//title
title = getTitle();
setBatchMode(true);
```

```
mpshape = newArray ("Fibers", "Fragments", "Micro-spheres");
for (i = 0; i < mpshape.length; i++) {
      selectWindow(title);
      run("Duplicate...", " ");
      rename(mpshape[i]);
}
run("Tile");

//Analyze Fibers
selectWindow(mpshape[0]);
run("Analyze  Particles...",  "size=3-1000000  pixel  circularity=0.0-0.3
display");

//Analyze Fragments
selectWindow(mpshape[1]);
run("Analyze  Particles...",  "size=3-1000000  pixel  circularity=0.3-0.6
display");

//Analyze Micro-spheres
selectWindow(mpshape[2]);
run("Watershed");
run("Analyze  Particles...",  "size=3-1000000  pixel  circularity=0.6-1.0
display");

//Get results and save to excel
for (i = 0; i < mpshape.length; i++) {
      close(mpshape[i]);
}
run("Original Scale");

//**Name of the saved file include the word Blue to differentiate it from
the one produced by the original script
dir = File.directory;
name = File.nameWithoutExtension;
saveAs("results",  dir + name + "_MP2resultsBlue.xls");
}

//If there is selection, delete unselected part
detsel = selectionType();
if (detsel==-1){
red();
mpvat();
}
```

```
else if (detsel>=0){
roiManager("Add");
setBackgroundColor(255, 255, 255);
run("Clear Outside");
roiManager("Delete");
red();
mpvat();
}
}
```

C. Appendix: Foraminifera plate

Figure C1. Examples of some individuals found for each morphology (see Figure 14). Categories according to chamber arrangement and coiling types. M1: miliolid coiling; M2: trochospiral coiling in spiral, and ventral views; M3: planispiral involute coiling in lateral and edge views; M4: biserial test; M5: triserial test; M6: uniserial test; M7: planispiral evolute coiling; M8: spiral to serial test; M9: single chambered test; M10: cyclic annular-discoidal test; M11: bi- to uniserial test; and M12: tests of the superfamily Soritoidea Ehrenberg, 1839.